

**UNCLASSIFIED**

CLASSIFICATION OF THIS PAGE

## REPORT DOCUMENTATION PAGE

AD-A205 089

DTIC  
-ECTE

1b. RESTRICTIVE MARKINGS

DTIC FILE COPY

2b. DECLASSIFICATION / DOWNGRADING DATE FEB 14 1989

4. PERFORMING ORGANIZATION REPORT NUMBER(S)

5. MONITORING ORGANIZATION REPORT NUMBER(S)

6a. NAME OF PERFORMING ORGANIZATION

OPTRA, Inc.

6b. OFFICE SYMBOL  
(If applicable)

7a. NAME OF MONITORING ORGANIZATION

U.S. Army Strategic Defense Command

6c. ADDRESS (City, State, and ZIP Code)

66 Cherry Hill Drive  
Beverly, MA 01915

7b. ADDRESS (City, State, and ZIP Code)

P.O. Box 1500  
Huntsville, AL 35807-38018a. NAME OF FUNDING / SPONSORING  
ORGANIZATION

U.S. Army Strategic Defense Command

8b. OFFICE SYMBOL  
(If applicable)

9. PROCUREMENT INSTRUMENT IDENTIFICATION NUMBER

DASG60-87-C-0019

8c. ADDRESS (City, State, and ZIP Code)

P.O. Box 1500  
Huntsville, AL 35807-3801

10. SOURCE OF FUNDING NUMBERS

PROGRAM  
ELEMENT NO.PROJECT  
NO.TASK  
NO.WORK UNIT  
ACCESSION NO.

11. TITLE (Include Security Classification)

Interferometric Optical Synchro for Alignment Transfer

12. PERSONAL AUTHOR(S)

Herman DeWeerd

13a. TYPE OF REPORT  
FINAL13b. TIME COVERED  
FROM 87/02/27 TO 88/11/2614. DATE OF REPORT (Year, Month, Day)  
89/02/0915. PAGE COUNT  
60

16. SUPPLEMENTARY NOTATION

17. COSATI CODES

FIELD

GROUP

SUB-GROUP

18. SUBJECT TERMS (Continue on reverse if necessary and identify by block number)

angle encoder, frequency laser, phase meter,  
nanoradian resolution, Michelson interferometer,  
zero mark generation, reflective grating. (jhd)

19. ABSTRACT (Continue on reverse if necessary and identify by block number)

Two 50 nanoradian resolution angle transducers were built employing laser interferometric techniques. Each encoder was provided with a reference or "zero" marker which employed a white light Michelson interferometer. The encoders were operated and the performance of one was evaluated in terms of the performance of the other in order to evaluate the suitability of the encoders for use in an optical synchro system for alignment transfer.

The specified angular resolution of 100 nanorad has been met with a performance of .43 nanorad resolution per root/Hz (10.5 nanorad at 600 Hz). The specification that requires one encoder to track the other within 100 nrad has been met by demonstrating that the second encoder will return to the zero reference position of the first encoder with 16 nrad (rms)/96 nrad (3σ).

20. DISTRIBUTION / AVAILABILITY OF ABSTRACT

☐ UNCLASSIFIED/UNLIMITED☐ SAME AS RPT.☐ DTIC USERS

21. ABSTRACT SECURITY CLASSIFICATION

UNCLASSIFIED

22a. NAME OF RESPONSIBLE INDIVIDUAL

Phil Williams

22b. TELEPHONE (Include Area Code)

(205) 895-3054

22c. OFFICE SYMBOL

CSSD-H-CRS

**UNCLASSIFIED**

**UNCLASSIFIED**

SECURITY CLASSIFICATION OF THIS PAGE

19. ABSTRACT (con't)

The encoders have been built as a self-contained device and is as such transportable. The implementation of the optical design is robust and we conclude that the encoder design is ready to be incorporated in a next higher level system, such as a combination of a reference platform/remote, slaved mirror. *Keywords. — to field?*

18. SUBJECT TERMS (con't)

Total Dollar Value \$468,165, Competitive Award



Accession For	
NTIS GRAM	J
DTIC TAB	
Unannounced	
Justification	
By	
Dist In	
Approved	
Dist	Source
F-5	

**UNCLASSIFIED**

SECURITY CLASSIFICATION OF THIS PAGE

FINAL REPORT  
(DRAFT)

SUBMITTED TO:

DEPUTY COMMANDER  
U.S. ARMY STRATEGIC DEFENSE COMMAND  
CONTR. & ACQ MGT. OFC, DASD-M-CRT  
P.O. BOX 1500, HUNTSVILLE, AL 35807-3801

CONTRACT NO: DASG60-87-C-0019

INTERFEROMETRIC OPTICAL SYNCHRO FOR ALIGNMENT TRANSFER

SUBMITTED BY:

OPTRA, INC.  
66 CHERRY HILL DRIVE  
BEVERLY, MA 01915

PROGRAM MANAGER: HERMAN DEWEERD

"The views, opinions, and/or findings contained in this report are those of the author(s) and should not be construed as an official Department of the Army position, policy, or decision, unless so designated by other official documentation."

"Further dissemination only as directed by the U.S. Army Strategic Defense Command, ATTN: DASD-H-MPL, P.O. Box 1500, Huntsville, AL 35807-3801, 1 April 1985, or higher DOD authority."

# OPTRA

**CERTIFICATION OF TECHNICAL DATA CONFORMITY (OCT 1985)  
(DFARS 52.227-7036)**

The Contractor, OPTRA, Inc. hereby certifies that, to the best of its knowledge and belief, the technical data delivered herewith under Contract No. DASG60-87-C-0019 is complete, accurate, and complies with all requirements of the contract.

2/10/89

Date



James R. Engel, President

## TABLE OF CONTENTS

<u>PARA</u>	<u>TITLE</u>	<u>PAGE</u>
1	SUMMARY.....	1
2	CONCLUSIONS.....	1
3	PRINCIPLE OF OPERATION.....	1
4	SYSTEM ANALYSIS.....	5
5	SYSTEM DESCRIPTION.....	7
6	PERFORMANCE EVALUATION.....	25
7	LESSONS LEARNED.....	26

## APPENDICES

APPENDIX A:	RADIOMETRIC ANALYSIS.....	A1
APPENDIX B:	VIBRATION ANALYSIS.....	B1
APPENDIX C:	LASER DESCRIPTION.....	C1
APPENDIX D:	PHASEMETER DESCRIPTION.....	D1
APPENDIX E:	TEST DATA.....	E1

## 1. SUMMARY.

Two 50 nanoradian resolution angle transducers were built employing laser interferometric techniques. Each encoder was provided with a reference or "zero" marker which employed a white light Michelson interferometer. The encoders were operated and the performance of one was evaluated in terms of the performance of the other in order to evaluate the suitability of the encoders for use in an optical synchro system for alignment transfer.

## 2. CONCLUSIONS.

The specified angular resolution of 100 nanorad has been met with a performance of .43 nanorad resolution per root/Hz (10.5 nanorad at 600 Hz). The specification that requires one encoder to track the other within 100 nrad has been met by demonstrating that the second encoder will return to the zero reference position of the first encoder with 16 nrad (rms)/96 nrad (3 $\sigma$ ).

The encoders have been built as a self-contained device and is as such transportable. The implementation of the optical design is robust and we conclude that the encoder design is ready to be incorporated in a next higher level system, such as a combination of a reference platform/remote, slaved mirror.

## 3. PRINCIPLE OF OPERATION.

3.1 Introduction. The angle transducer employs a Moire based signal modulation for the angle encoding and a differing Michelson interferometer for the zero pulse generator. The Moire pattern is generated by a traveling pattern of laser interference fringes and the rulings of a radial grating. The latter is configured as a lateral motion sensor located at a certain radius from a point of rotation of the grating.

### 3.2 Principle of the Measurement of the Angular Motion.

3.2.1 Interferometric Detection of Lateral Motion. Figure 3.1 shows the layout for interferometrically detecting lateral motion. Two laser beams, derived from the same laser, are incident at an angle  $\theta$  at a point P on a diffracting surface. In the region in which the two beams overlap, an interference fringe pattern is formed as shown. The fringe spacing  $d$  is given by:

$$(3.1) \quad d = w/2\sin\theta,$$

where  $w$  is the wavelength of the laser. When the surface moves, the grating rulings on its surface pass through the spatially modulated intensity pattern and produce a temporally modulated scattered intensity with a frequency  $f$ :

$$(3.2) \quad f = v/d = 2v (\sin\theta)/w,$$

where  $v$  is the velocity component in the plane of the surface and perpendicular to the interference fringes. By detecting this intensity modulation the lateral velocity of the surface can be monitored; its displacement can be arrived at by integrating the velocity ( $dx = vdt$ ).

The scenario described above suffers from two defects. In particular, low frequency intensity modulations of the laser--or of the detector current--can be misinterpreted as surface displacements, and the method cannot sense the sign of the motion. Both of these difficulties can be overcome by using a 2-frequency laser. The output from a 2-frequency HeNe OPTRALITE™ laser is comprised of two superimposed beams which are orthogonally polarized, and which differ in frequency by 250 KHz.

Figure 3.1 shows the arrangement for detecting lateral motion with a 2-frequency laser. The two frequency components are separated with a polarizing beamsplitter (not shown), and are superposed on the surface. An interference fringe pattern is formed in the region of beam overlap and, because of the frequency difference between the two laser beams, the fringes are not stationary: they move in a direction normal to the fringes and pass by fixed points on the surface at a frequency  $f_d = f_2 - f_1$ , where  $f_2$  and  $f_1$  are the frequencies of the two laser beams (the fringes move toward the laser beam with the lower frequency).

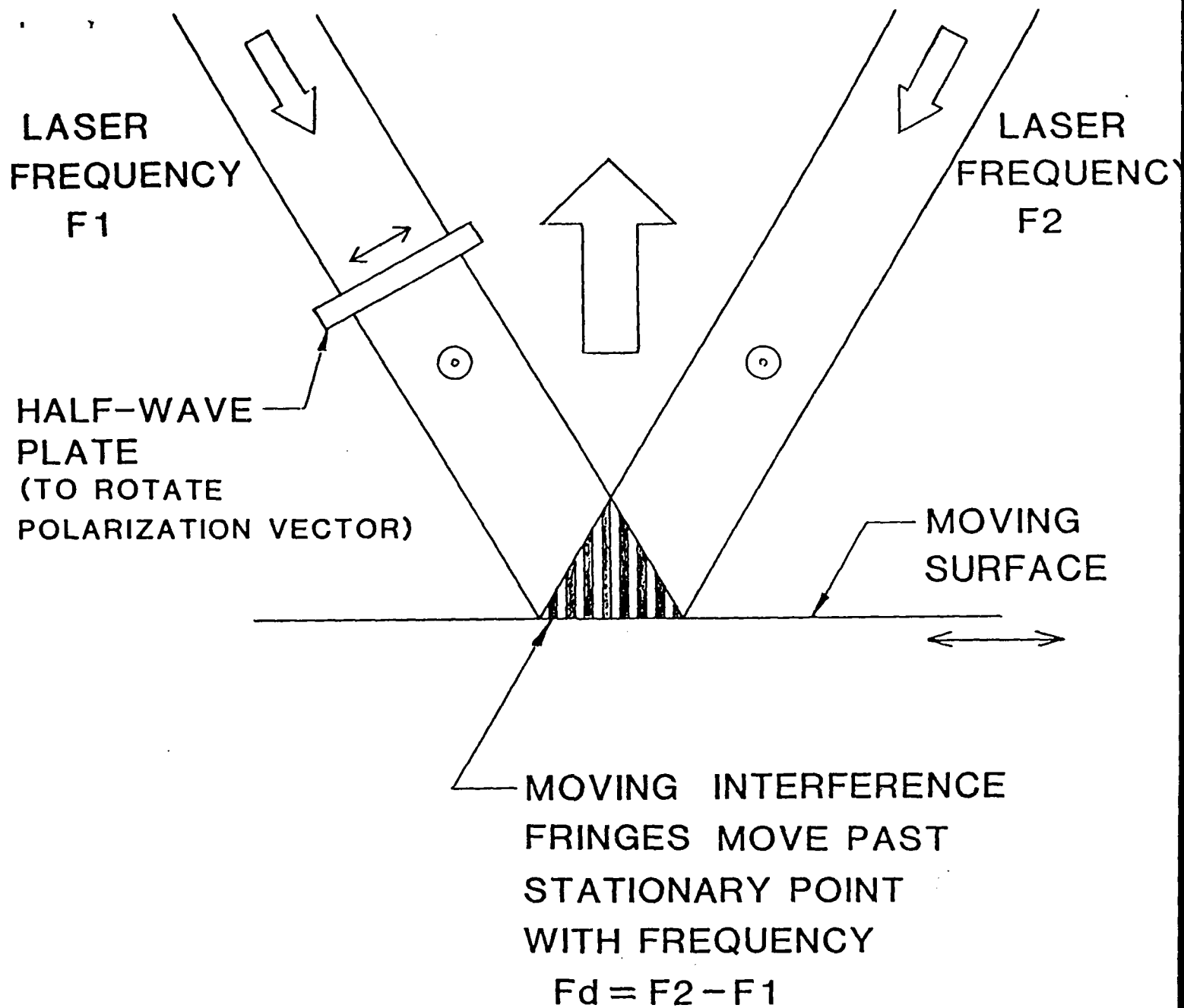
When the surface is stationary the diffracted light is modulated at the laser difference frequency. When the surface moves, the modulation frequency of the diffracted light is shifted due to the motion of the surface:

$$(3.3) \quad f = f_d \pm (2v(\sin\theta))/w,$$

where the sign on the right side of the equation depends on whether the surface is moving against or with the fringe motion.

The advantages of this approach are: (1) the direction of motion is unambiguously sensed; and (2) all of the detected frequencies are in the vicinity of the laser difference frequency; low frequency laser intensity fluctuations are thus virtually eliminated as a source of noise in the measurement. Moreover, the motion of the surface can be easily monitored by detecting the phase difference between the laser difference frequency (detected at the rear of the laser) and the detected modulation of the light diffracted by the surface. For each distance  $d$  ( $d = w/2\sin\theta$ ) the surface moves, this phase difference is incremented (or decremented) by 1 full cycle. That is:

$$(3.4) \quad n = x/d,$$



- ⊙ VERTICALLY POLARIZED  
 ↔ HORIZONTALLY POLARIZED

Fig. 3-1

The interference fringes are created in the area where the two laser beams intersect.



where  $n$  is the total number of cycles and  $x$  is the total displacement. The system employed an OPTRA designed phase meter which has a dynamic range limited only by the choice of electronic components, is capable of easily resolving better than 0.001 cycle, and has a measurement bandwidth in excess of 20 KHz.

**3.2.2 Measurement of Angular Motion.** In order to infer an angular velocity from a measurement of transverse displacement, it is only necessary to know the displacement of the point of measurement from the axis of rotation. The tangential velocity of the grating surface at the point of measurement is  $R(dA/dt)$ , where  $dA/dt$  is the angular velocity of the shaft (radians/sec). Using this information in combination with equations (3.1) and (3.4) gives a relationship between the detected phase difference (between the diffracted signal and a static reference) and the angle  $A$  through which the shaft has rotated and is given by:

$$(3.5) \quad \text{phase difference} = AR/d = 2AR\sin\theta/w,$$

where  $A$  is measured in radians and the phase difference is measured in cycles. For the 22.33 degree angle of incidence and a 13 cm grating radius, the fringe spacing is 0.833 MM.

It is at this point not possible to distinguish between angular rotation and small lateral (tangential) motions of the grating. In order to eliminate the sensitivity to translation, a second interferometer is required on the opposite side of the shaft from the first. The optical path is arranged so that the same optical frequency is transmitted by the beamsplitter on both sides. The phase of the signal from each interferometer will shift identically with any lateral movement of the shaft. However, a rotation of the shaft causes the signal phases to change in opposite directions. Hence, if the phase difference between these two interferometer signals is monitored, the phasemeter output will represent pure rotation, independent of small translations of the shaft. Furthermore, the detected light modulation is no longer referenced to the laser difference frequency, but the modulations on the two interferometers are intra-referenced, thus doubling the angular resolution in the process.

The phase change of one interferometer signal is represented by equation (3.5); the phase change from the second interferometer signal (also with respect to a static reference) is given by:

$$(3.6) \quad \text{phase change} = -2AR\sin\theta/w,$$

and the phase difference between the two interferometer signals as measured by the phasemeter is:

$$(3.7) \quad \text{phase difference} = 4AR\sin\theta/w.$$

3.3 Principle of Generating the Zero Position Signal. The zero marker design employs the classical Michelson interferometer with the moving reflector attached to the edge of the encoder disk. Each mirror is mounted on a piezo-electric driver.

The signal from the white light fringe is differentiated by dithering the interferometer mirrors which are mounted on the piezo actuators. This generates an AC signal which is either in phase or 180° out of phase with the dithering frequency, except at zero path difference. By synchronously detecting the AC component, referenced to the dithering frequency, a DC voltage proportional to the slope of the white light fringe is generated. The zero reference position of the encoder disk is sharply defined at the point where the slope crosses the zero volt coordinate.

#### 4. SYSTEM ANALYSIS.

The system design is modeled as shown in table 4-1. The results of the system analysis were as follows:

$$\text{LSB}_{\text{ERROR}} = 16 \text{ Nanoradians}$$

$$\text{Signal}_{\text{ERROR}} = 0.262 \text{ Nanoradians (14.9 mW signal)}$$

$$\text{Ref}_{\text{ERROR}} = 0.748 \text{ Nanoradians (1.83 mW signal)}$$

$$\begin{aligned} \text{TOTAL SIGNAL} &= \sqrt{(16)^2 + (.262)^2} = 16 \\ \text{ERROR} \end{aligned}$$

$$\begin{aligned} \text{TOTAL REF} &= \sqrt{(16)^2 + (.748)^2} = 16 \\ \text{ERROR} \end{aligned}$$

$$\begin{aligned} \text{TOTAL ERROR} &= \sqrt{(\text{REF})^2 + (\text{SIGNAL})^2} \\ &= \sqrt{(16)^2 + (16)^2} \end{aligned}$$

$$\text{TOTAL ERROR} = 22.6 \text{ Nanoradians}$$

The detailed analysis is given in Appendix A.

- \* 1 MHz measurement bandwidth.
- 256 sample average.
- 50% modulation efficiency.
- Shot-noise limited.

# LATERAL MOTION METROLOGY WITH REFLECTIVE GRATING

-> OPTICAL SYNCHRO 31-Jul-87

Inputs<	Fringe spacing	0.83 microns	0.000032 inches
	Resolution elem./fringe	128	
	Laser power	5.0E-04 watt	
	System transmission	0.2	
	Detector X-dimension	2 mm	0.078740 inches
	Detector Y-dimension	2 mm	0.078740 inches
	Stand-off distance	2 cm	0.787401 inches
	X-spot dimension	165 microns	0.006496 inches
	Y-dimension/X-dimension	1.0	
	Wavelength	6.3E-05 cm	2.48E-05 inches
	Grating efficiency	0.25	
	Grating reflectance	0.90	0.000035 inches
	Grating radius	13 cm	
	Detector/preamp NEP	1.00E-12 watt/rt.Hz	
	Measurement bandwidth	1000 Hz	
	Mean spot diameter	0.165 mm	0.064960 inches
	Angle between beams	44.4 degrees	
	Beam separation at head	1.63 cm	0.643281 inches
	Depth of focus	0.12 mm	0.004639 inches
	Power at detector	2.3E-05 watt	
	Lateral resolution	0.0065078 microns	
	Angular resolution	0.0501 microrad	0.000002 deg
	Signal power	2.3E-05 watt	
	Sig/Elec.noise	7.1E+05	
	Sig/ShotNoise	2.7E+05	

Table 4-1  
System model

## 5. SYSTEM DESCRIPTION.

The system consists of three major assemblies, namely the sensor head, containing the two shaft encoder opto-mechanical units, the two OPTRAMETER™ phasemeters, and the control display electronics unit. (See system block tree figure 5-1)

**5.1 Sensor Head.** The conceptual opto-mechanical design of the encoder heads was directly affected by the specification to "demonstrate that one encoder can track the other within 100 nrad". With the performance of the transducers being initially unknown, it was necessary to rotate the shaft of each encoder by a known angle to a resolution of less than 100 nrad. There are two potential ways in which to do this, namely to employ an alternate set of calibrated encoders or to couple the two shafts mechanically to each other. The former option is not available for obvious reasons. The most practical way to implement the latter is to build the two encoders on a common shaft.

The sensor head therefore consists of a frame (box, see Figure 5-1) which supports a spindle assembly comprised of a shaft, two encoder disks, two pairs of reading head laser interferometers, and a zero marker white light interferometer for the master disk.

**5.1.1 Optical Diagram.** The optical diagram shown in Figure 5-2 is identical for both encoders. The diagram is characterized by its simplicity; it lends itself to be packaged as a rugged, interchangeable module.

**5.1.2 Mechanical Design.** With increasing resolution in rotation and other sensors, perturbations caused by thermal and vibration effects increasingly adversely affect the capability to perform the high resolution measurement. Considerable attention was therefore paid to analyzing these effects so that the theoretical optical resolution would not be lost.

**5.1.2.1 Thermal Design.** Differential temperatures in the encoder head assembly may effect system performance in three ways, namely de-focus, and radial and tangential shifts between the reading heads and the disks.

The depth of focus of the reading head is .433mm (0.17"); this is a rather large number in light of the given thermal stability and thermal effects on focus will not be analyzed.

A differential tangential shift will cause a false rotation read-out. It is difficult to conceive how a differential tangential shift will develop because of the symmetrical nature of the layout. Although the performance of the system is linearly sensitive to tangential shift (a 0.2 micro inch differential shift corresponds to 50 nanorad), the thermal effect on tangential shift will not be analyzed.

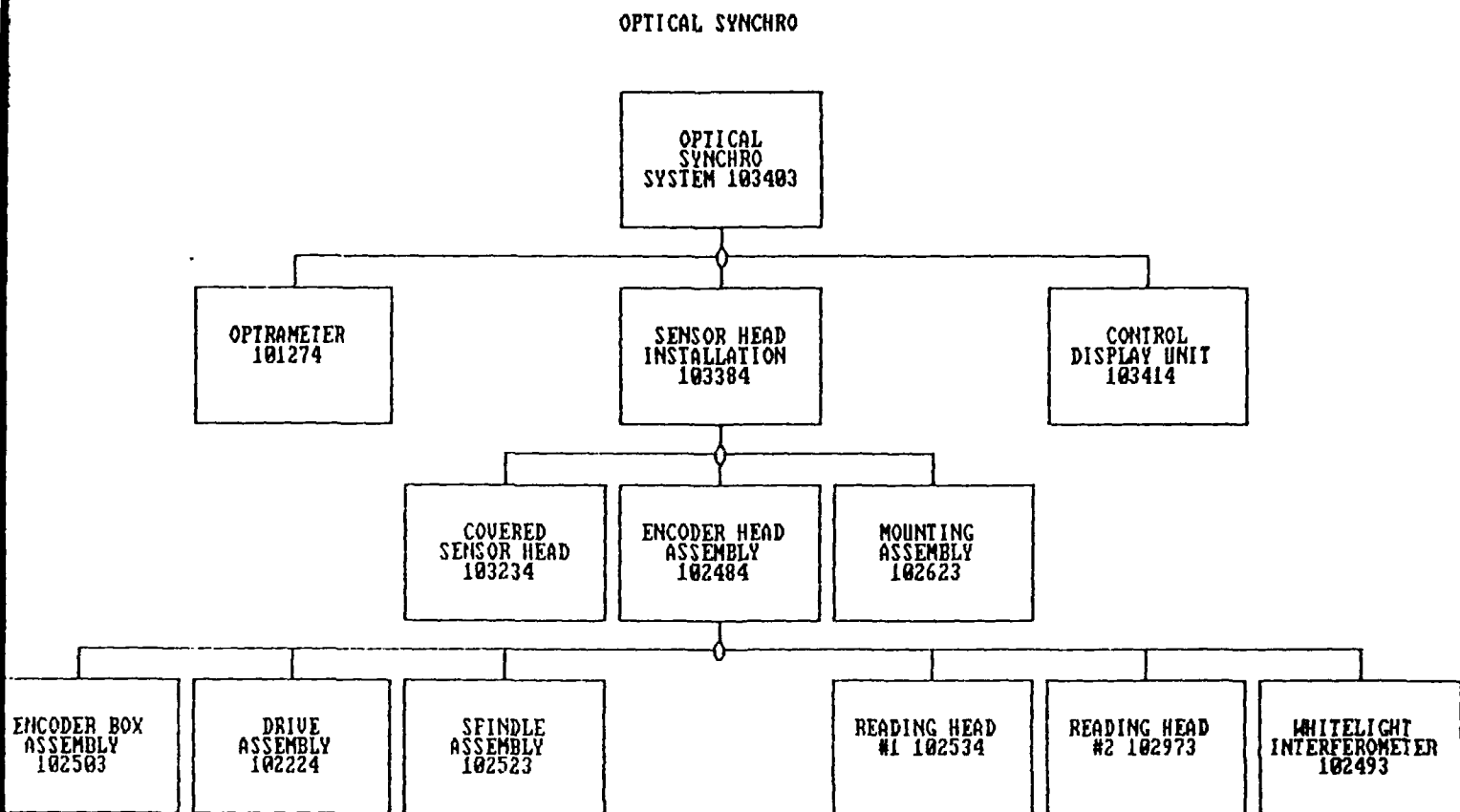


Fig. 5-1  
System block tree

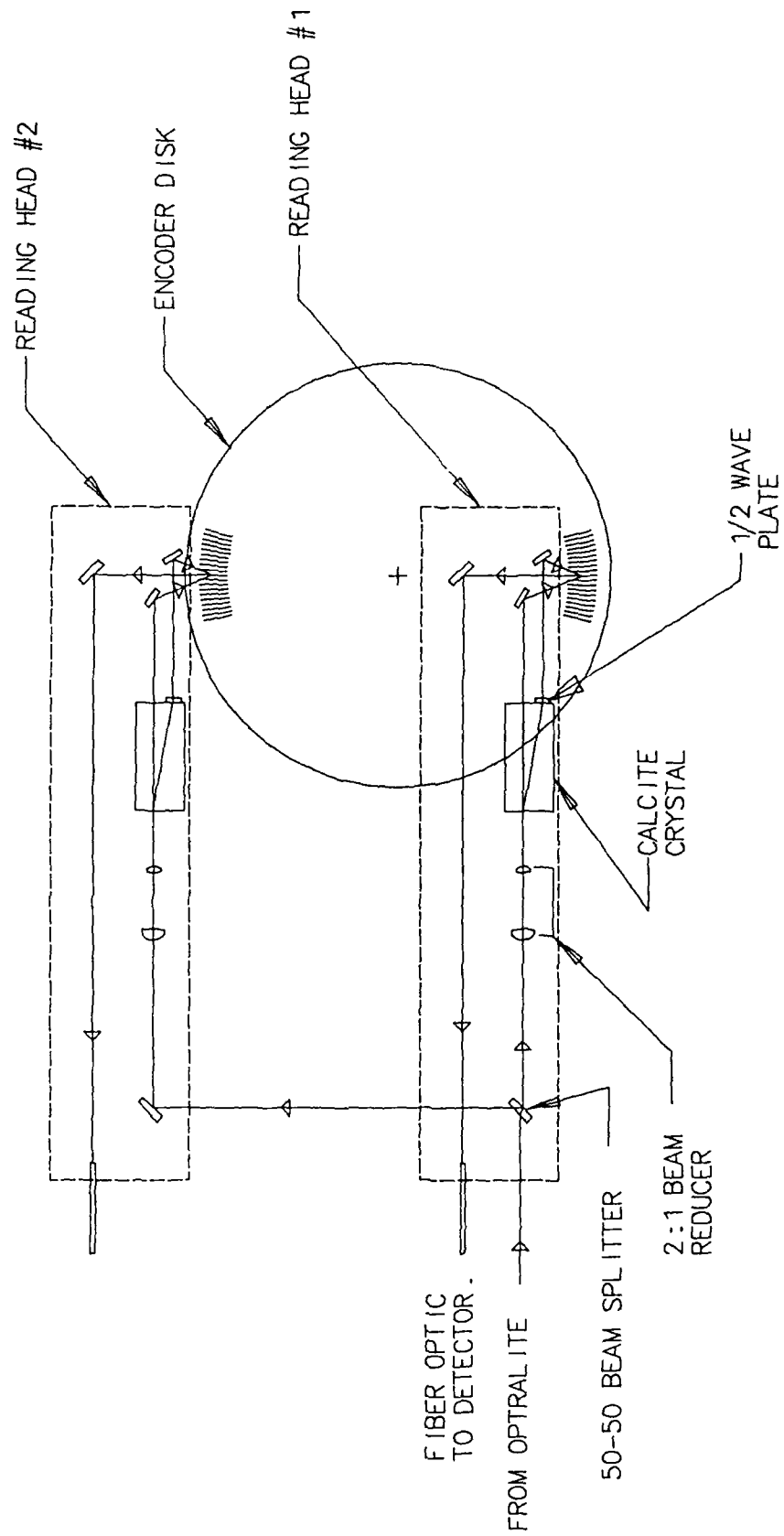


FIGURE 5-2

A radial shift of the reading head with respect to the disk will change the number of working grating lines per mm and will have an effect on the transfer function of the system and on the modulation efficiency. The thermal effect on the transfer function and the modulation efficiency are analyzed below. Such a shift would be caused, if heat would enter the frame from the front (or back) causing the front to expand away from the shaft, while the disk would lag. The effects of heat on the system transfer function and modulation efficiency are as follows:

#### A. THERMAL EFFECT ON TRANSFER FUNCTION.

The sensitivity of the angular accuracy to change in the working radius is 50 nanorad/.22 microinch over a 5° angle of rotation.

The CTE of Invar is given as  $(.96 \text{ to } 1.08) \times 10^{-6}/^{\circ}\text{C}$ . A .051°C temperature rise in the front half of the frame will cause a beam-across-disk shift of .22 microinch.

Such a rise in temperature requires .347 BTU. The sensitivity of the angular accuracy to temperature is: 50 nanorad/.051°C and to heat: 50 nanorad/.347 BTU.

#### B. THERMAL EFFECT ON MODULATION EFFICIENCY.

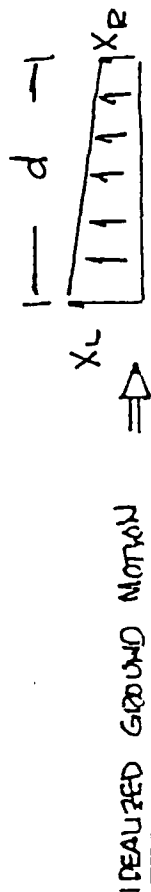
The sensitivity of the modulation efficiency to changes in the dimension of the working radius (number of lines/mm) is such that the m.e. will be 50% when the beam spot has shifted .0018".

These numbers above show that the subject transducers are quite sensitive to sources of heat as small as that of a human body. The sensor head will therefore be enclosed by a thermal shroud to shield it from short term thermal transients that may present themselves in the experiment's room. We are striving here for thermal stability only, not operation at a certain temperature; active thermo-statted temperature control is necessary. And finally, the frame of the head will be constructed out of Invar, because its CTE is approximately 6 times smaller than that of aluminum, thus making a thermally more stable structure.

5.1.2.2 Vibration Analysis. The sensor head was installed on a MICRO-G air table. The source of the vibration is the floor of the room.

Ground motion is essentially random. Hence, each leg of the table is subjected to a random vibration input which results in non-uniform or angular rotation of the table. For the purpose of the analysis, the ground is idealized as a harmonic input having a uniform lateral ( $\delta$ ) and rotational component ( $\sigma$ ).

The optical synchro is more sensitive to the angular component than the uniform component of the idealized ground motion. Note that an angular ground rotation of 1 arc sec (5 micro radians)



$$\varphi = \varphi_0 \sin \pi t \quad (\text{ANGULAR COMPONENT})$$

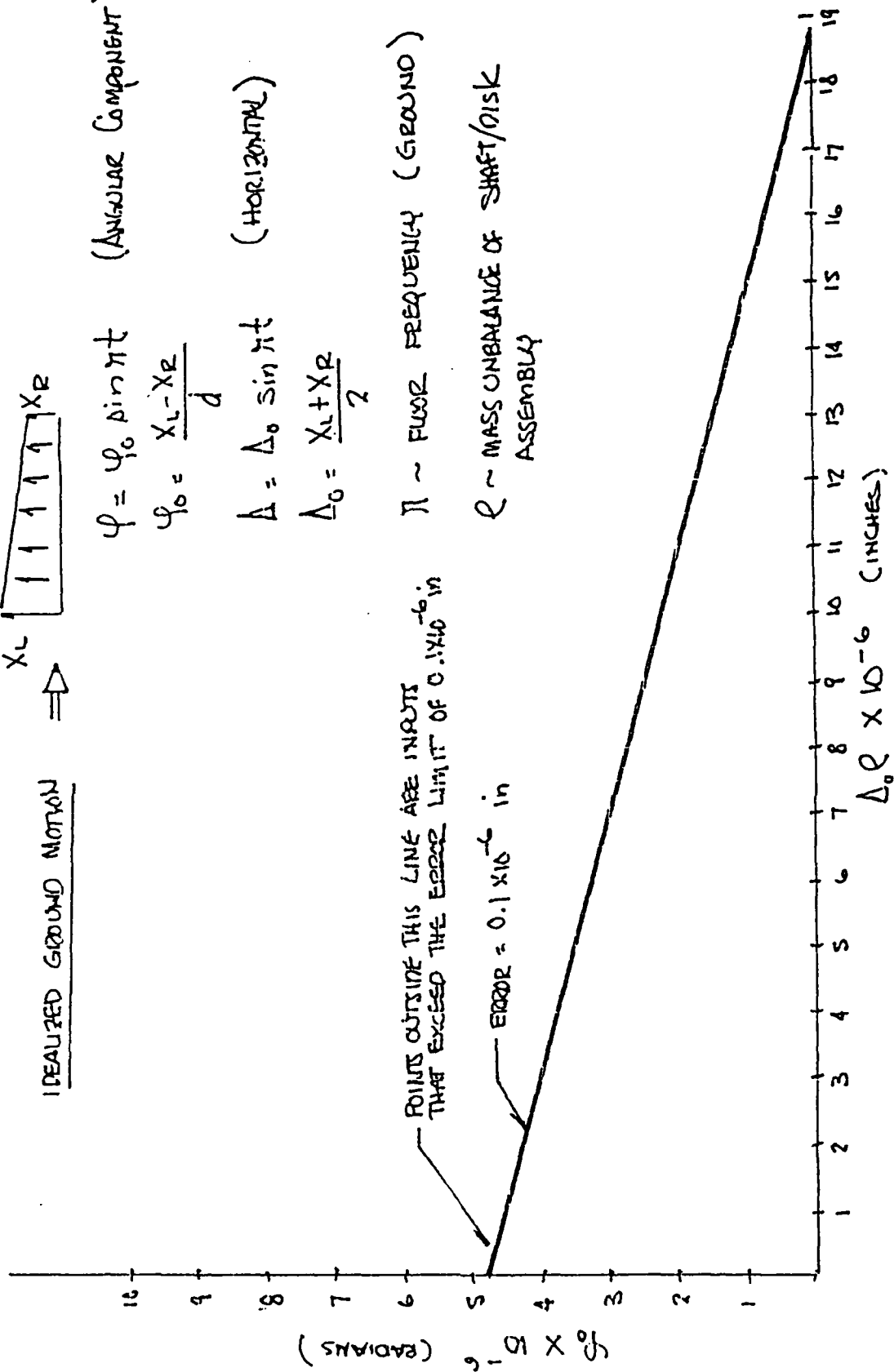
$$\varphi_0 = \frac{X_L - X_R}{d}$$

$$A = A_0 \sin \pi t \quad (\text{HORIZONTAL})$$

$$A_0 = \frac{X_L + X_R}{2}$$

$\pi \sim$  FLOOR FREQUENCY (GROUND)

$\rho \sim$  MASS UNBALANCE OF SHAFT/DISK ASSEMBLY



UNIFORM HORIZONTAL COMPONENT

Rotational ground vibration

FIG 5-2a



will produce an error of 0.1 micro inch. The uniform horizontal component results in an error only if the shaft/disk assembly and/or the isolation system is unbalanced. For ground motions in the order of 0.1 mils a shaft unbalance of nearly 0.2 inches would result in an error of 0.1 micro inches.

**5.1.2.3 Mechanical Configuration.** The concept of the angle encoding sensor consists in employing an 8" diameter disk which is encoded with a radial grating and projecting onto the grating at two places 180° apart a moving fringe pattern which is generated by two optical heads fed by an OPTRALITE two-frequency laser (see Appendix C). Upon rotation of the disk, the reflected optical signal will be modulated and is sensed by detectors and processed in phasemeters and data handling electronics to yield the angle over which the disk has rotated. A separate white light interferometer is included to sense the reference or null position of the disk. The layout of this interferometer is shown in Figure 5-3.

In the electro-optical system design, the phase shift in the signal from one optical head is compared with that of the other head, thus doubling the angular resolution and rendering the system insensitive to translation of the disk with respect to the heads. The two heads are therefore fed by a single laser source. The beam is split 50-50 and subtended to the interferometer in each head. The layout of the optical heads is shown in Figure 5-4.

The encoded disk is attached to a hub which is mounted on a shaft via a clamp and radial position adjustments (see Figure 5-5); the latter will enable us to center the disk on the axis of rotation of the shaft. Figure 5-5 shows the two disks mounted to a common shaft. The disks (see Figure 5-6) were procured from Hyperfine, Inc., in Boulder, Colorado.

The shaft/disk assembly, the  $2 \times 2 = 4$  optical heads, and the white light interferometer are attached to an Invar frame (see Figure 5-7). The frame is enclosed in a isothermal box, to prevent environmentally induced thermal transients from reaching the sensor head; it is mounted on a vibration isolated table, to prevent ground vibrations from reaching the sensor head.

The means by which the shaft is rotated and held in place merits careful attention. An improperly fixed shaft may give rise to false readings. The shaft itself is supported by two balls in order to attain true rotation around a center line. The shaft is coupled via a five degree-of-freedom coupling to a fine-advance arm, which also acts as the clamped arm in the hold mode (see Figure 5-8). The fine-advance arm is driven by a piezo electric driver, which is anchored to a coarse-advance arm; the latter is in turn driven by a high precision micrometer head.

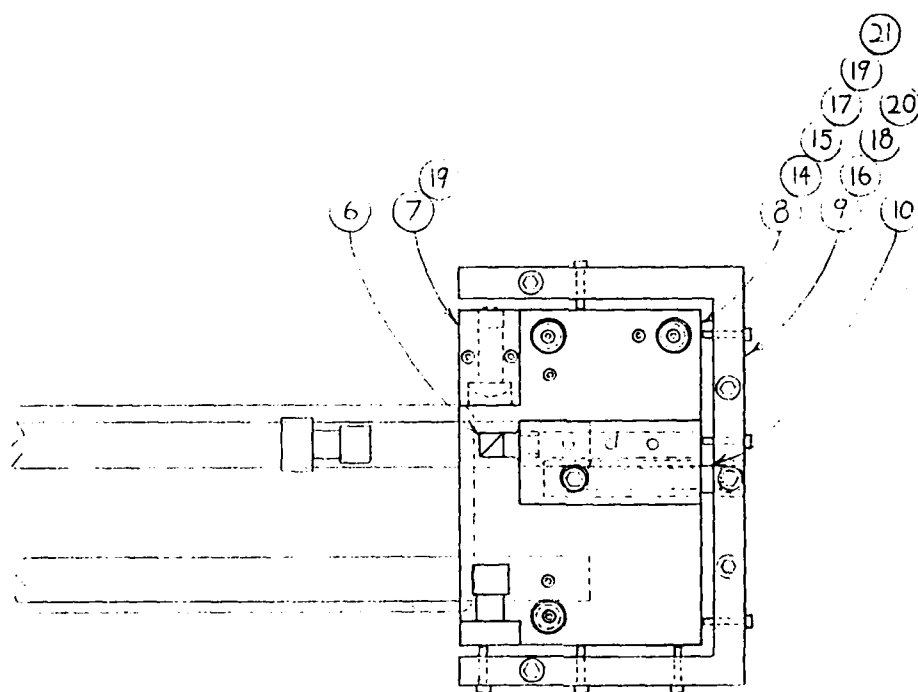
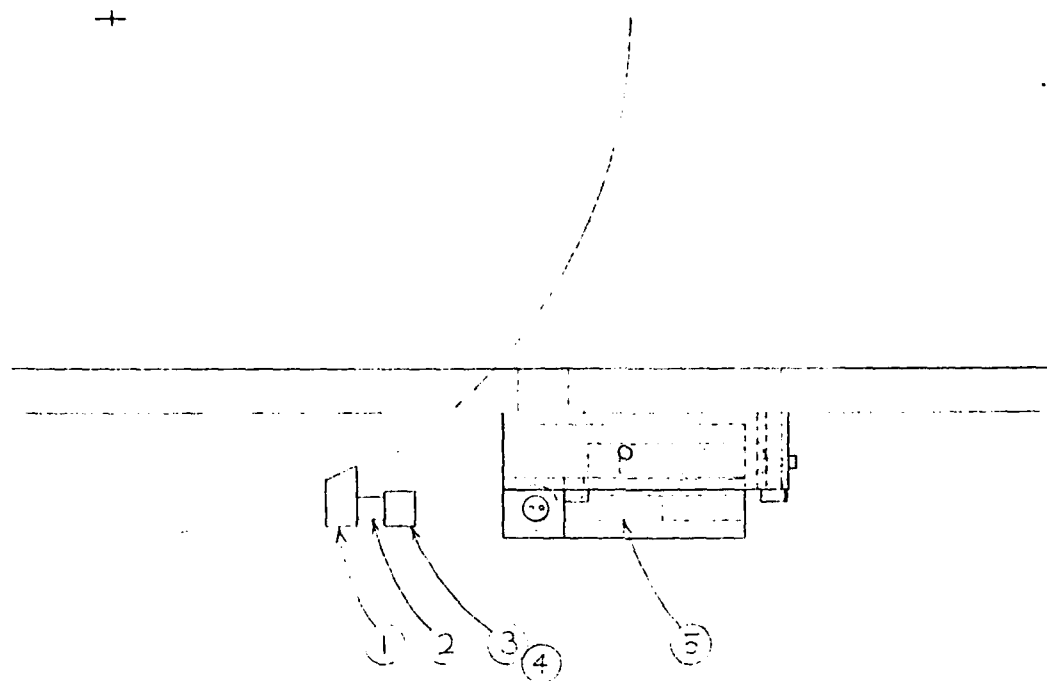


FIGURE 5-3  
WHITE LIGHT INTERFEROMETER LAYOUT

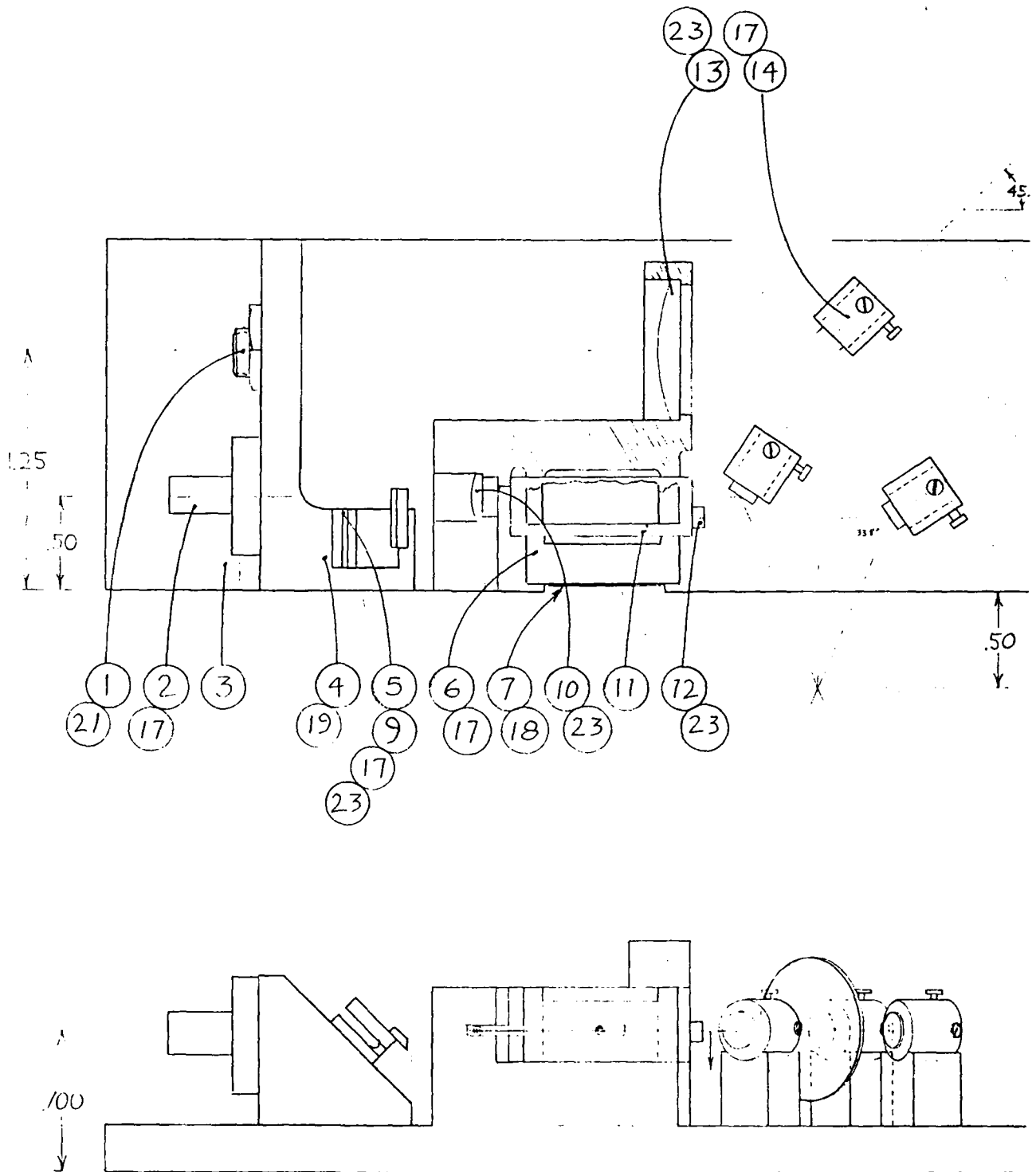


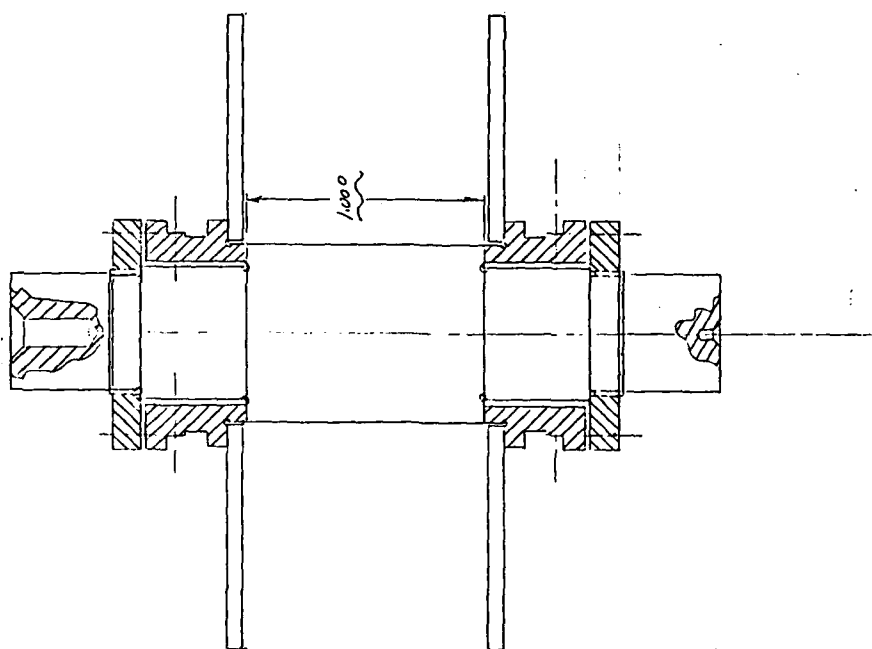


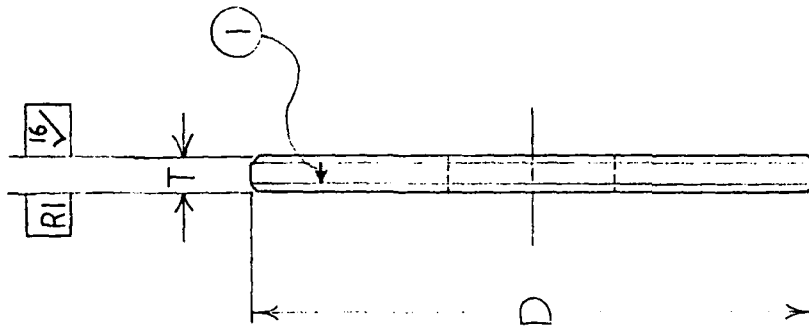
FIGURE 5-4  
OPTICAL HEAD LAYOUT

MAIL	FINISH	<div><div></div><div>SURFACE UNLESS SHOWN OTHERWISE</div></div>										<div><div></div><div>SPINDLE ASSEMBLY</div></div>									
		DOWN	SMALL	CHUB	SMALL	APPRO	SMALL														
		INCHES	4	IN	UNLESS SHOWN OTHERWISE	INCHES	4	IN	UNLESS SHOWN OTHERWISE	INCHES	4	IN	UNLESS SHOWN OTHERWISE	INCHES	4	IN	UNLESS SHOWN OTHERWISE	INCHES	4	IN	
		MILLIMETERS	100	1	2	10	1	2	10	1	2	10	1	2	10	1	2	10	1	2	
		TITLE																			
		PAGE NO	1, 02, 52, 3, 00																		
		DATE																			
		TIME																			
		REMARKS																			
		AND BREAK AWAY																			
		SHARP EDGES																			
		SCALE																			

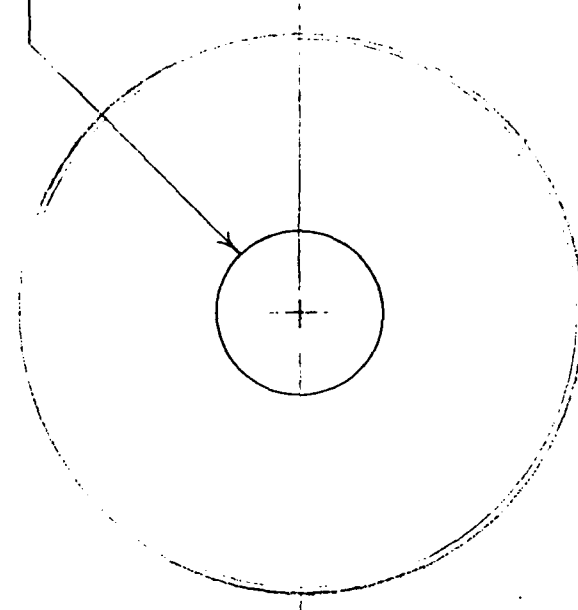


DIMENSIONS INCH	SIDE 1	SIDE 2
RADIUS OF CURVATURE	R1	R2
RADIUS TOLERANCE	N/A	N/A
FRINGE TOLERANCE	4	N/A
IRREG. TOLERANCE	1	N/A
FINISH	80-60	N/A
COATING	NONE	NONE
CLEAR AP. DIAMETER	218.0	N/A
SAGITTA		S2
DIA. TO FACE		Y2
DIA. TO BEVEL		
FACE WIDTH TO BEVEL		D2
BEVEL WIDTH	C1	C2
FACE ANGLE	0.5x45°	0.5x45°
THICKNESS	TH	9.53
TH. TOL.	± .2	
WEDGE TOL.	1.5°	
FLAT TIR		
DIAMETER	DIA	219.0
DIA. TOL.	± 1.0	
MATERIAL	FUSED SILICA	
GRADE	NOTE 2	

REV	DESCRIPTION	BY	DATE
01			
02			



60.325 DIA  
THRU,  
Ø .010 TIR



NOTE 1: INDICATE SURFACE R1 WITH  
ARROW IN THE EDGE  
NOTE 2: ULE OR EQUIVALENT

MATERIAL:		OPTRA				83 PINE STREET PEABODY, MA 01960 (617) 535-7670				NEXT ASSY DWG NO.	
FINISH:		DWN	DATE	CHKD	DATE	APPD	DATE	10247400			
SURFACE:		63	DIMS ARE:		TOL. UNLESS SHOWN OTHERWISE						
UNLESS SHOWN OTHERWISE		X = 1.0		X = 2		XX = .10					
TITLE		GRATING BLANK									
REMOVE BURRS AND BREAK ALL SHARP EDGES		DWG NO.		4 012		1 01		SH 1 OF		REV.	
SCALE: 1:1											

FIGURE 5-6a  
ENCODER DISK

REV	DESCRIPTION	DATE
01	NOTES GENERALLY UPDATED	11/18/84
02		

# NOTES:

## 1. RULED AREAS (2):

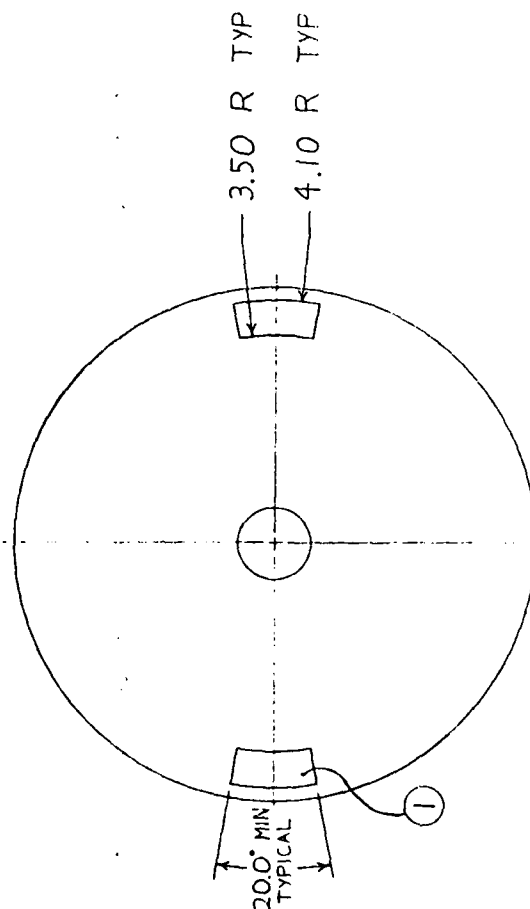
- 1.1 LINE DENSITY: 600  $\frac{\text{lines}}{\text{mm}} \pm 2 \frac{\text{lines}}{\text{mm}}$  NOMINAL AT RADIUS OF 4.00 NOMINAL.
- 1.2 CONSTANCY OF GROOVE SPACING TO BE  $\pm 0.6 \%$  OR BETTER AT A RADIUS WHICH IS CONSTANT TO  $\pm 0.001$  OR BETTER.
- 1.3 GROOVE ORIENTATION: RADIAL
- 1.4 GROOVE CONFIGURATION:

- A: TO BE OPTIMIZED FOR MAX DIFFRACTION INTO  $\pm$  AND  $\pm$  FIRST ORDERS OF NORMAL INCIDENCE, 632.8 nm LIGHT BEAM. THE DIFFRACTION IS TO BE BY REFLECTION
- B: AMOUNT OF ENERGY DIFFRACTED INTO  $\pm$  1ST ORDER TO BE EQUAL TO AMOUNT OF ENERGY DIFFRACTED INTO  $\pm$  1ST ORDER WITHIN 10%.

## 1.5 RULING MATERIAL: TBD BY VENDOR.

## 2. PROVIDED BY OPTRA (DWG # 40119101).

## 3. PROTECTIVE $\text{SiO}_2$ OVERCOAT CONSISTENT WITH PARA. 1.4



MATERIAL: NOTE 2		83 PINE STREET PEABODY, MA 01960 (617) 535-7670		NEXT ASSY DWG NO.	
FINISH:	DATE	CHKD	DATE	APPD	DATE
NOTE 3	11/19/87		11/19/87		10247400
SURFACE: 63		DIMS ARE: TOL UNLESS SHOWN OTHERWISE ANGLES = 1°			
UNLESS SHOWN OTHERWISE		INCHES X = 05 XX = 010			
		MILLIMETERS X = 2.54 XX = 2.54			
		TITLE			
		RADIAL REFLECTION GRATING			
REMOVE BURRS AND BREAK ALL SHARP EDGES		DWG NO.		REV	
		40119101		SH 1 OF 1	
SCALE: 1:1					

FIGURE 5-6b Encoder Disk

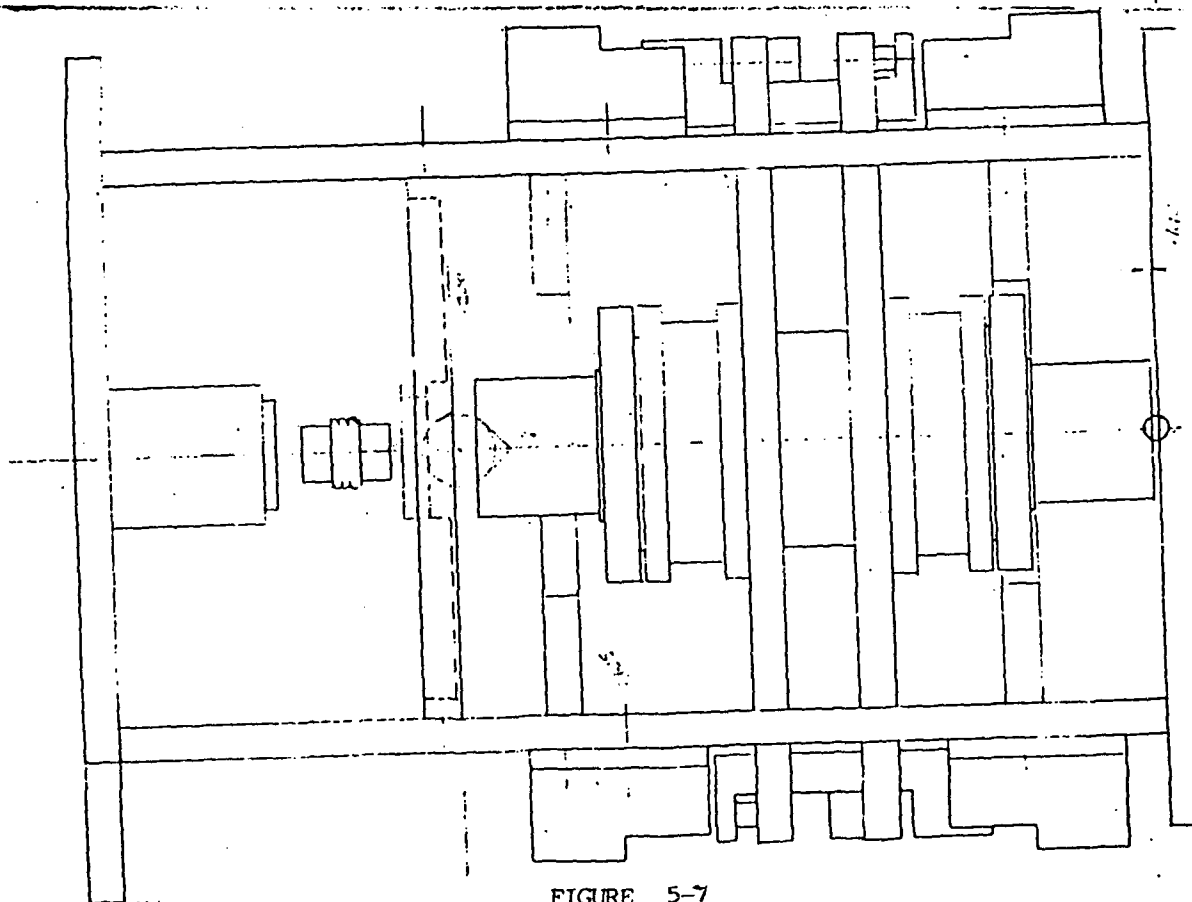
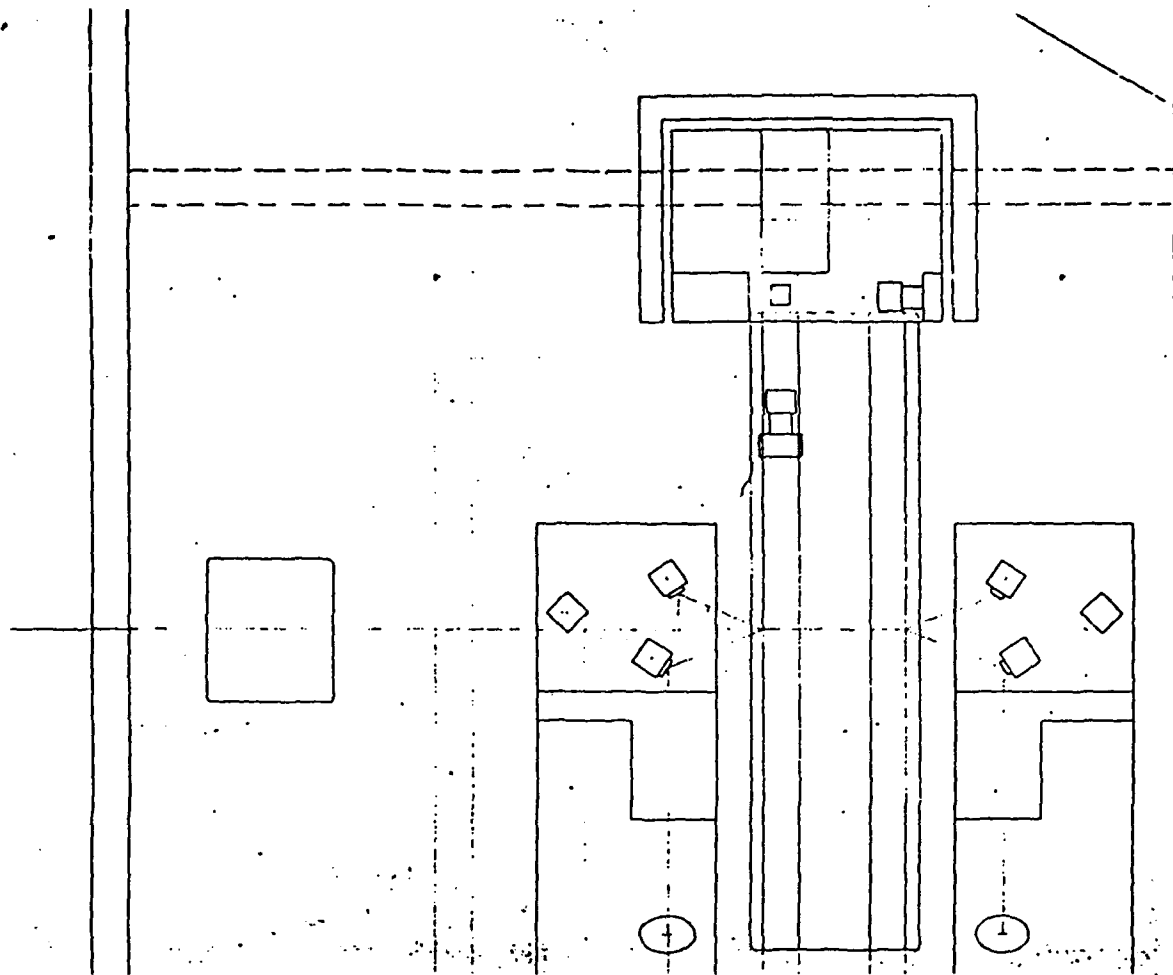
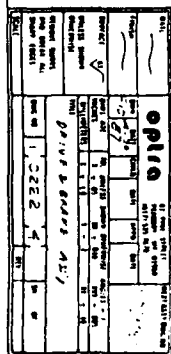


FIGURE 5-7  
SENSOR HEAD LAYOUT



1	2	3	4	5	6	7	8	9	10	11	12	13	14	15	16	17	18	19	20	21	22	23	24	25	26	27	28	29	30	31	32	33	34	35	36	37	38	39	40	41	42	43	44	45	46	47	48	49	50	51	52	53	54	55	56	57	58	59	60	61	62	63	64	65	66	67	68	69	70	71	72	73	74	75	76	77	78	79	80	81	82	83	84	85	86	87	88	89	90	91	92	93	94	95	96	97	98	99	100
---	---	---	---	---	---	---	---	---	----	----	----	----	----	----	----	----	----	----	----	----	----	----	----	----	----	----	----	----	----	----	----	----	----	----	----	----	----	----	----	----	----	----	----	----	----	----	----	----	----	----	----	----	----	----	----	----	----	----	----	----	----	----	----	----	----	----	----	----	----	----	----	----	----	----	----	----	----	----	----	----	----	----	----	----	----	----	----	----	----	----	----	----	----	----	----	----	----	----	-----



5.2 Phasemeter. Each transducer employs a standard OPTRAMETER™ phasemeter to detect and accumulate the fringes and to measure and display the fringe phase. The phasemeter is described in Appendix D.

5.3 Control and Display Electronics Unit. The Optical Synchro Electronics consists of standard and custom designed assemblies that display the angular position of 2 encoders, controls the white light interferometer, generates zero marks and stores and displays the angular position of both encoders when a zero mark is generated. Figure 5-9 is a block diagram of the Optical Synchro Electronics.

5.3.1 Detector Assemblies. The angular position of each encoder is determined by a standard OPTRAMETER™ and detector assemblies. The inputs to the detector assemblies are the optical signals from the encoder coupled through fiber optics. The outputs of the detector assemblies are nominal 250 kHz sine waves. The detector assembly characteristics are:

gain	$3 \times 10^6$	volt/watts
bandwidth	25 kHz to 1MHz	
N.E.P.	$5 \times 10^{-13}$	watt/(Hz) <sup>1/2</sup>

Nominal modulated input signals from the encoders are 1 microwatt P-P (or mW pp).

5.3.2 Display Electronics. The Display Electronics consist of mode select logic circuits and latched displays which store and display the 2 OPTRAMETER outputs when the white light interferometer generates a zero mark. The logic circuits are controlled by pushbuttons on the Control/Display unit front panel. The pushbuttons enable the storage circuits. When a zero mark occurs the 2 OPTRAMETER outputs ( $\pm 9.999$  fringes) are stored. Front panel LEDs indicate the circuits status (enabled, data stored).

5.3.3 White Light Interferometer Electronics. The white light interferometer electronics include all circuits required to generate a zero mark, when the encoder position is at the white light interferometer zero path difference ( see Figure 5-10, block diagram). The basic approach used is to differentiate the white light fringe (see Figure 5-11) detected by a germanium detector and transimpedance amplifier, and detect when the differentiated fringe is at zero which occurs when the interferometer is at its zero path difference. A window comparator is used to detect the zero condition. When the window comparator zero conditions are met and the DC signal from the transimpedance amplifier is at a maximum one millisecond pulse is generated by a one-shot which is the zero mark.

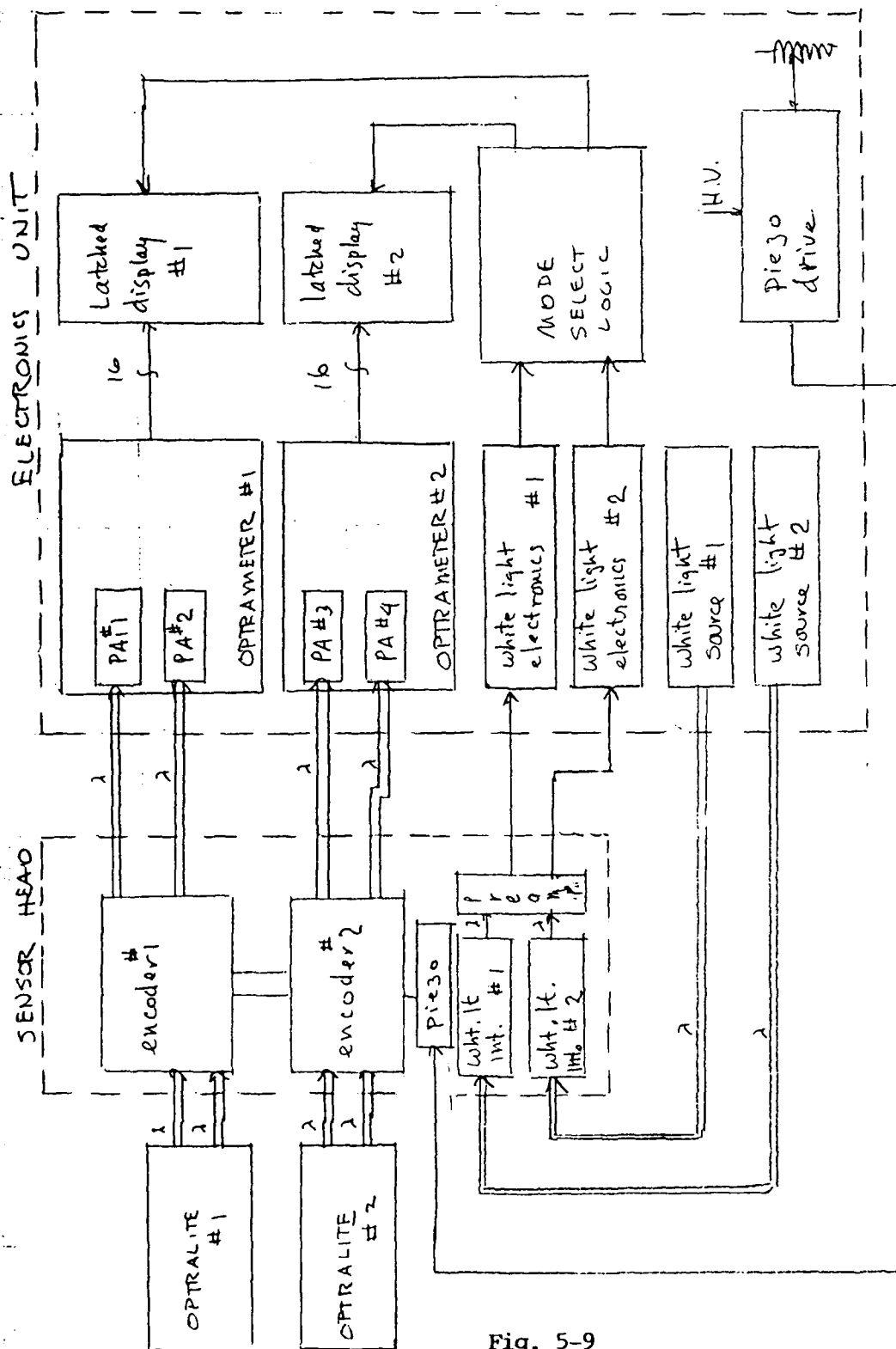


Fig. 5-9  
System block diagram



Both traces  
Y: 400mv/DIV

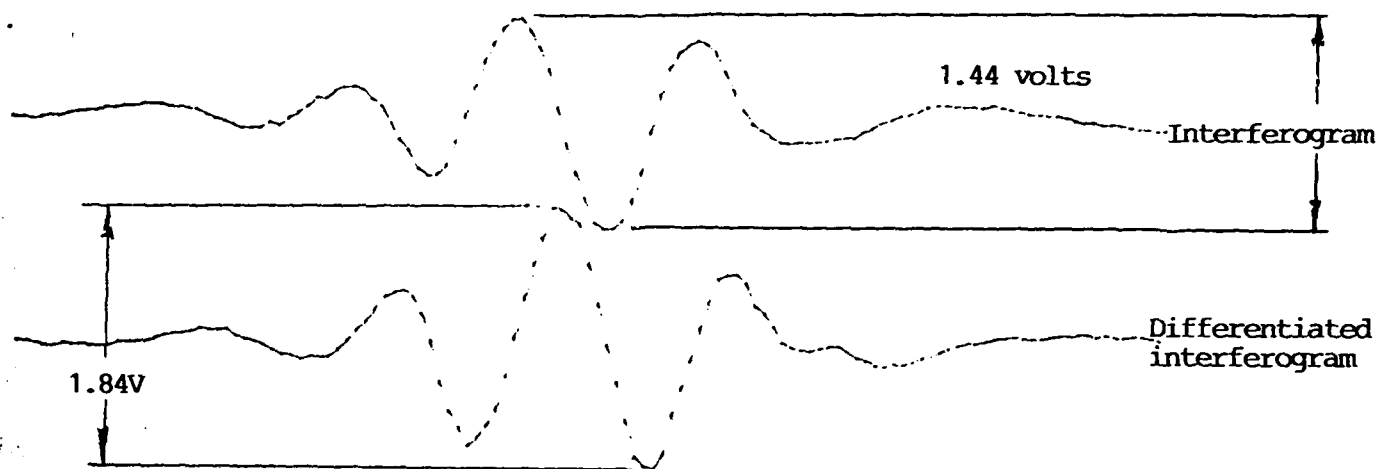


Fig. 5-11

Zero mark interferometer signals  
Note that the maximum fringe is the black fringe

5.3.4 Piezo Drive. The encoders are moved via a lever arm on which is mounted a piezo actuator. Fine control of the encoder position is realized by driving the piezo actuator with a variable DC voltage ranging from 0 to -1000 VDC. The Servo Control Circuit provides a 10 turn potentiometer which adjusts a high voltage supply from 0 to -1000 VDC.

## 6.0 PERFORMANCE EVALUATION.

The performance was evaluated for two parameters, namely the angular resolution and the accuracy with which the slave transducer would return to the zero position as defined by the master transducer.

6.1 Resolution. In order to be able to demonstrate that the slave would be able to follow the master to within 100 nrad, it was necessary to design and build each transducer with a resolution of less than 50 nrad. As no suitable test facility was available against which to determine the resolution, this performance parameter is derived by design:

the resolution  $\{x = \frac{d}{R \times N \times 2}$ , where

$d$  = fringe spacing =  $\lambda/2 \sin\theta = 633/2 \sin 22.33^\circ$

$R$  = working radius of the encoder disk

$N$  = bits/fringe

2 = the result of two reading heads,  $180^\circ$  apart

$$\{x = \frac{8.33 \times 10^{-7}}{1.3 \times 10^{-1} \times 256 \times 2} = 12.5 \text{ nrad}$$

The transducers were designed for a resolution substantially less than 50 nrad, because we were striving for 3 $\sigma$  performance in the tracking test.

6.2 Tracking Test. In the tracking test, both master and slave were driven through the master-zero position and the bit count of each transducer was strobed at that position and recorded. Both disks were then rotated over an arbitrary angle, the bit count was noted at the stop position, and the disks were returned to the master-zero position where the bit count was again strobed and recorded. The following data that was collected is shown in Appendix E.

The average zero position error is:

for the master transducer:  $1.25/46 = +.027$  bits

for the slave transducer:  $1.43/46 = +.031$  bits

The error between master

and slave tracking is: .004 bits

The system scale factor is 4 nrad = .001 bit i.e.

The tracking error is 16 nrad (1 $\sigma$ ) or 96 nrad (3 $\sigma$ )

## 7.0 LESSONS LEARNED.

Below follows an evaluation of a number of aspects of the design in terms of actual performance. It is noted that the negative lessons (paragraph 7.2, 7.3, and 7.4) are peripheral issues that do not affect the actual sub 100 nrad metrology.

### 7.1 The Metrology Concept.

The concept of employing a laser interferometer generated fringe pattern in conjunction with a radially ruled grating to resolve rotation of less than 100 nrad has proven to be entirely sound and practical. The concept, reduced to hardware, yielded a robust system that is ready to be incorporated in a next higher level system in the field.

The concept of employing a Michelson interferometer too, including the diffracted mirrors has proven to be practical and the hardware functioned well.

7.2 Fiber Optic Links. The optical output of each of the four laser interferometers was collected by a multi-strand optical fiber cable and conducted to the respective detector-preamp units in the phasometers. These fiber optic links performed satisfactorily.

The design incorporated originally a single mode fiber between the two lasers and the two transducers. These fibers were built, but we were unable to obtain a satisfactory performance (i.e. polarity crosstalk free) within the budget and schedule constraints. As this problem has been solved in several places elsewhere, it is not a problem that cannot be fundamentally overcome.

7.3 Shaft Drive. The hand operated micrometer drive proved as convenient to operate as the piezo drive was, attaining the same finesse, therefore, we did not use the piezo drive except at the initial stages of the testing effort.

The drive showed noticeable hysteresis indicating that more attention should have been paid to the drive mechanism of the spindle. We particularly suspect the bellows coupling between the drive shaft and the disk spindle to be a major contribution to this problem.

7.4 Signal Jitter. It was not feasible to fix the disk/reading head system such that the display showed no rotation. Rather, the display showed a constant jitter, indicating that even with the drive brake activated, the system was not truly fixed. This is not a trivial problem and it is not surprising that we had to cope with it in light of the limited scope of the encoder.

## APPENDIX A RADIOMETRIC ANALYSIS

The radiometric analysis reveals that there is plenty of light in the Optical Synchro design. The analysis reveals that system resolution is limited by the number of bits used per fringe (128). I recommend increasing to 256 bits per fringe.

Last, it is important that the bandwidth of the electronics be reduced to 8.5 kHz and that you really do average 250 samples per measurement. Otherwise this analysis will be invalid, and you will no longer have an abundance of light.

### OPTICAL SYNCHRO RADIOMETRIC ANALYSIS

This report is organized into the following sections:

1. Determination of Key Variables
2. Optical Schematic
3. Tabulation of Component Efficiencies (Signal Path)
4. Analysis (Signal Path)
5. Tabulation of Component Efficiencies (Reference Path)
6. Analysis (Reference Path)
7. Fringe Counting Analysis

#### DETERMINATION OF KEY VARIABLES:

- Maximum velocity: 2 radians/minute
- Grating: 600 lines/millimeter
- Radius: 4 inches = 101.6 mm

- Doppler shift:

$$2 \frac{\text{RAD}}{\text{MIN}} \cdot \frac{2 \cdot (101.6 \text{ mm})}{2 \cdot \text{Radians}} \cdot \frac{600 \text{ Lines}}{\text{MM}} \cdot \frac{\text{MIN}}{60 \text{ SEC}} = 2032 \frac{\text{Lines}}{\text{Sec}}$$

2.03 kHz

- Total Doppler Shift: 4.06 V 1/2
- Preamp Noise Bandwidth: 8.5 kHz
- Detector/Preamp Noise  $\approx 3.3 \times 10^{-13}$
- Update Rate: 1 kHz
- Number of samples per measurement (N):

$$\frac{250 \text{ kHz}}{1 \text{ KHz}}$$

$$= 250$$

- Fringe Radians vs. Shaft Radians:

2" Shaft Radians  
2" (101.6 MM)

MM  
600 Fringes

Fringe  
2" Fringe  
Radians

$$= \frac{2.61 \times 10^{-6} \text{ Shaft Radians}}{1 \text{ Fringe Radians}}$$

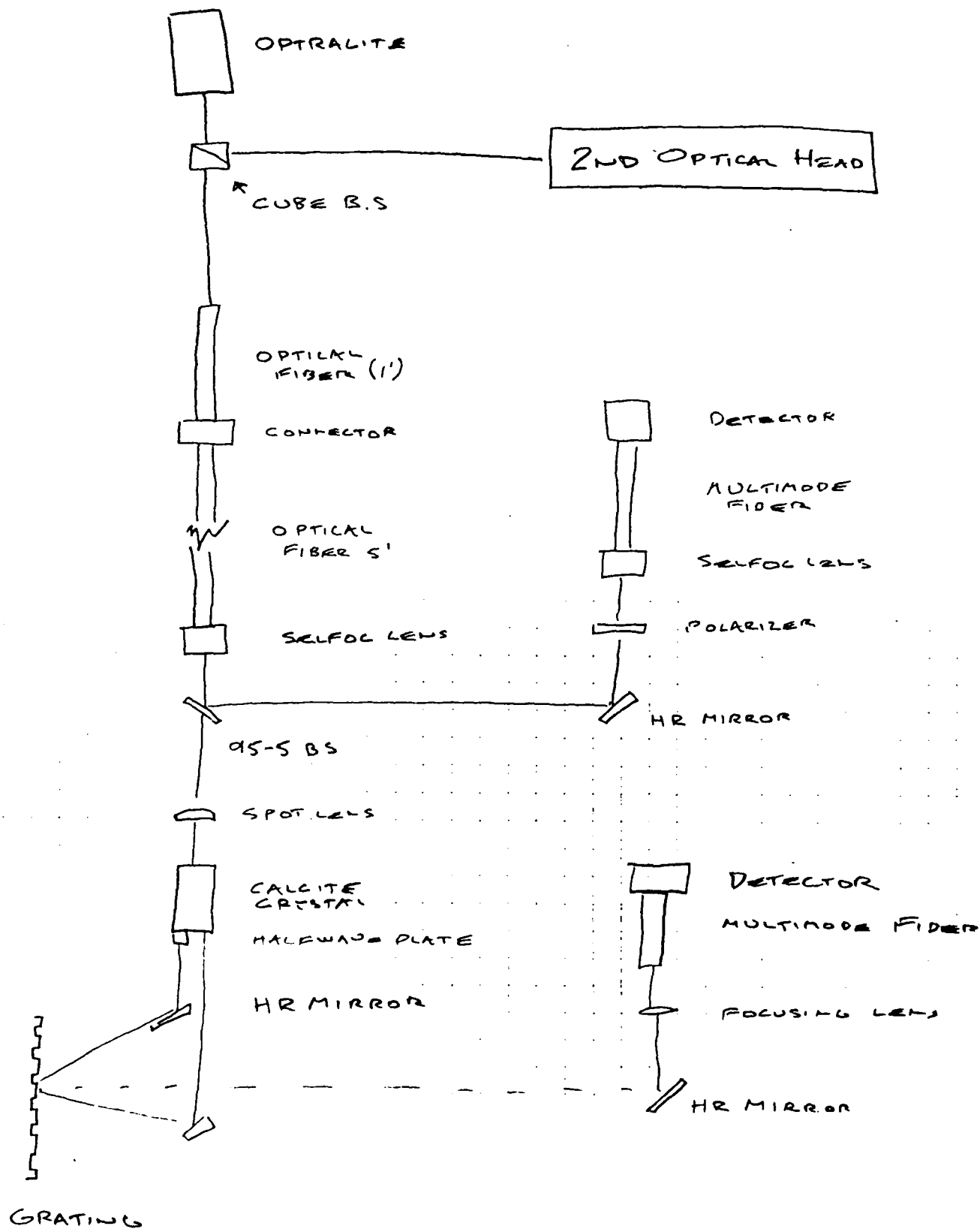
### 3. TABULATION OF COMPONENT EFFICIENCIES (SIGNAL PATH)

<u>COMPONENT</u>	<u>EFFIC</u>	<u>CUM EFF</u>
Optralite		
Cube B.S.	.40	
Coupling into Fiber	.70	.28
Connector	.70	.196
Selfog Lens	.95	.186
BS (.95 x .90)	.855	.159
Spot Lens	.95	.151
Calcite Crystal	.95	.144
Half Wave Plate	.95	.136
HR Mirror	.90	.123
Diffraction Grating	.25	.0307
HR Mirror	.90	.0276
Focusing Lens	.95	.0263
Coupling to Fiber	.70	.0184
Along Fiber	.90	.0165
Out of Fiber	.90	.0149

LASER POWER =  $1 \times 10^{-3}$  W  
 $W_s$  P-P =  $(1 \times 10^{-3} \text{ W}) (.0149)$   
 $W_s$  P-P =  $1.49 \times 10^{-5} \text{ W}$



## 2) OPTICAL SCHEMATIC



#### 4) ANALYSIS (SIGNAL PATH)

LSB ERROR:

ERROR<sub>LSB</sub> =  $\frac{1}{2}$  AN LSB FOR A ONE HEAD SYSTEM.

ERROR<sub>LSB</sub> =  $\frac{1}{4}$  AN LSB FOR A TWO HEAD SYSTEM.

$$\left[ \text{LSB} = \frac{1}{128} \text{ FRINGE} \right]$$

$$\text{ERROR}_{\text{LSB}} = \frac{1}{4} \cdot \frac{\text{FRINGE}}{128} \cdot \frac{2\pi \text{ FRINGE RADIALS}}{\text{FRINGE}} \cdot \frac{2.61 \times 10^{-6} \text{ SHAFT RADIALS}}{\text{FRINGE RADIALS}}$$

$$= 3.2 \times 10^{-8} \text{ SHAFT RADIALS}$$

$$= \boxed{32 \text{ NANORADIALS}}$$

NOISE ERROR: FOR EXPLANATION OF THIS ANALYSIS, cf DC's 4/22/87 MEMO "TERADYNE SIGNAL REQUIREMENTS"

$$W_{N \text{ P-P}} = \text{NEP} \cdot (\text{NOISE BW})^{\frac{1}{2}} \cdot \left( \frac{6V_{PN}}{V_{\text{RMS}}} \right) \cdot \frac{1}{\sqrt{N}}$$

$$= \left( \frac{3.3 \times 10^{-13} \text{ WATT}_{\text{RMS}}}{\sqrt{\text{Hz}}} \right) \sqrt{8500 \text{ Hz}} \cdot \frac{6V_{PN}}{1V_{\text{RMS}}} \cdot \frac{1}{\sqrt{250}}$$

$$W_{N \text{ P-P}} = 1.15 \times 10^{-11} \text{ WATT}_{\text{P-P}}$$

$$\text{NOISE}_{\text{FRINGE RADIALS}} = \frac{2 \text{ FRINGE RADIALS}}{W_{S \text{ P-P}}} \cdot W_{N \text{ P-P}}$$

$$\text{NOISE}_{\text{SHAFT RADIALS}} = \frac{2 \text{ FRINGE RAD}}{W_{S \text{ P-P}}} \cdot W_{N \text{ P-P}} \cdot \frac{2.61 \times 10^{-6} \text{ SHAFT RADIALS}}{\text{FRINGE RADIALS}}$$

$$= \frac{(2)(1.15 \times 10^{-11})}{(1.49 \times 10^{-5})} \cdot (2.61 \times 10^{-6})$$

$$= 4.03 \times 10^{-12} \text{ SHAFT RADIALS}$$

$$= \boxed{0.004 \text{ NANORADIALS}}$$

$$\text{Total Signal Error} = \sqrt{\text{LSB}_{\text{error}}^2 + \text{Noise}_{\text{error}}^2}$$

$$= \sqrt{32^2 + .004^2}$$

$$= \boxed{32 \text{ NAUORADIANS}}$$

# 5) TABULATION OF COMPONENT EFFICIENCIES (REFERENCE PATH)

<u>COMPONENT</u>	<u>EFFICIENCY</u>	<u>CUMULATIVE EFFICIENCY</u>
OPTICALITE		
CUBE B.S.	.40	.40
COUPLING INTO FIBER	.70	.28
CONNECTOR	.70	.196
SELFOL LENS	.95	.186
B.S. (90% of 5%)	.045	.00838
H.R. MIRROR	.90	.00754
POLARIZER	.45	.00339
SELFOL LENS	.95	.00322
COUPLING TO FIBER	.70	.00226
ALONG FIBER	.90	.00203
OUT OF FIBER	.90	.00183

$$\text{LASER POWER} = 1 \times 10^{-3} \text{ W}$$

$$W_{\text{S.P.P}} = (1 \times 10^{-3} \text{ W})(.00183)$$

$$W_{\text{S.P.P}} = 1.83 \times 10^{-6} \text{ W}$$

## 6) ANALYSIS (REFERENCE PATH)

IDENTICAL TO SIGNAL PATH ANALYSIS EXCEPT THAT "PREAMP NOISE BANDWIDTH" CAN BE REDUCED TO 2 KHZ.

$$\text{ERROR}_{\text{LSB}} = 32 \text{ NANORADIANS}$$

NOISE ERROR:

$$W_{N.P-P} = (3.3 \times 10^{-13}) \sqrt{2000} (6) \frac{1}{\sqrt{250}}$$

$$= 5.60 \times 10^{-12} \text{ WATTS}_{P-P}$$

$$\text{NOISE}_{\text{SHAFT RADIALS}} = 2 \text{ FRINGE RAD.} \cdot \frac{W_{N.P-P}}{W_{S.P-P}} \cdot \frac{2.61 \times 10^{-6} \text{ SHAFT RADIAN}}{\text{FRINGE RADIALS}}$$

$$= \frac{2 (5.60 \times 10^{-12})}{(1.83 \times 10^{-6})} \cdot (2.61 \times 10^{-6})$$

$$= 1.60 \times 10^{-11} \text{ RADIALS}$$

$$\text{NOISE} = .016 \text{ NANORADIANS}$$

$$\text{TOTAL REFERENCE ERROR} = \sqrt{(32)^2 + (.016)^2}$$

$$\text{TOTAL REFERENCE ERROR} = 32 \text{ NANORADIANS}$$

$$\begin{aligned} \text{TOTAL POSITION ERROR (BOTH HEADS)} &= \sqrt{(\text{REFERENCE ERROR})^2 + (\text{SIGNAL ERROR})^2} \\ &= \sqrt{(32)^2 + (32)^2} \end{aligned}$$

$$\text{TOTAL POSITION ERROR (BOTH HEADS)} = \pm 45 \text{ NANORADIANS}$$

7)

## FRINGE COUNTING ANALYSIS

FOR EXPLANATION OF THIS ANALYSIS cf DC's  
4/22/87 MEMO "TERADYNE SIGNAL REQUIREMENTS"

- PEAK TO PEAK NOISE VOLTAGE MUST BE LESS THAN 10% OF COMPARATOR HYSTERESIS:

$$W_{N_{P-P}} = (3.3 \times 10^{-3}) \sqrt{8500} \text{ G} = 1.825 \times 10^{-10} \text{ WATTS}_{P-P}$$

$$\text{MIN HYSTERESIS IS: } 1.825 \times 10^{-9} \text{ WATTS}_{P-P}$$

- HYSTERESIS MUST BE LESS THAN 10% OF PEAK-PEAK SIGNAL:

$$\text{MIN } W_{S_{P-P}} = 1.825 \times 10^{-8} \text{ WATTS}_{P-P}$$

SINCE SIGNAL IS  $1.49 \times 10^{-5} \text{ WATTS}_{P-P}$  WE  
HAVE A 1000 X FACTOR OF SAFETY.

## APPENDIX B: VIBRATION ANALYSIS

### 1.0 FUNDAMENTAL FREQUENCY OF OPTICAL SYNCHRO

The optical synchro has a torsional resonance at 29 HZ in which the shaft/disks assembly rotates relative to the structural housing. The fundamental frequency is primarily controlled by the torsional stiffness of the bellows and the mass moment of inertia of the shaft/disk assembly. The housing may be considered rigid relative to the shaft/disk assembly since all remaining frequencies are significantly higher than 29 HZ.

### 2.0 ISOLATION SYSTEM

The optical synchro is isolated from ground motion by means of a MICRO-G air-operated vibration isolator. The horizontal frequency of the isolator reported by the manufacturer is 4 HZ. Using the manufacturer's recommended minimum of (4 HZ); the dynamic characteristics of the isolation system were evaluated based on a table weight of 150 lbs. Adding four 80 lb weights at the corners of the table will reduce the horizontal frequency to approximately 2 HZ. No attempt, however, was made to evaluate the effect of adding the four weights on the performance of the isolation system, and the table...\*

### 3.0 THE DYNAMIC MODEL

A two degree of freedom model is used to determine the dynamic response of the system to ground motion. Degree of freedom (1) represents the absolute angular rotation of the disk. Degree of freedom (2) represents the absolute rotation of the housing. Because the synchro housing is rigid relative to the shaft/disk assembly, it is assumed that the motion of the housing is identical to that of the table. The error is the relative rotation of degree of freedom (1) with respect to (2) times radius of disk:

$$\text{Error} = \{ (1) - \theta(2) \} r$$

\* The rated capacity of the table is 1400 lb. Total load is 150 + 320 + 95 = 465 lb.

### 4.0 DYNAMIC ANALYSIS

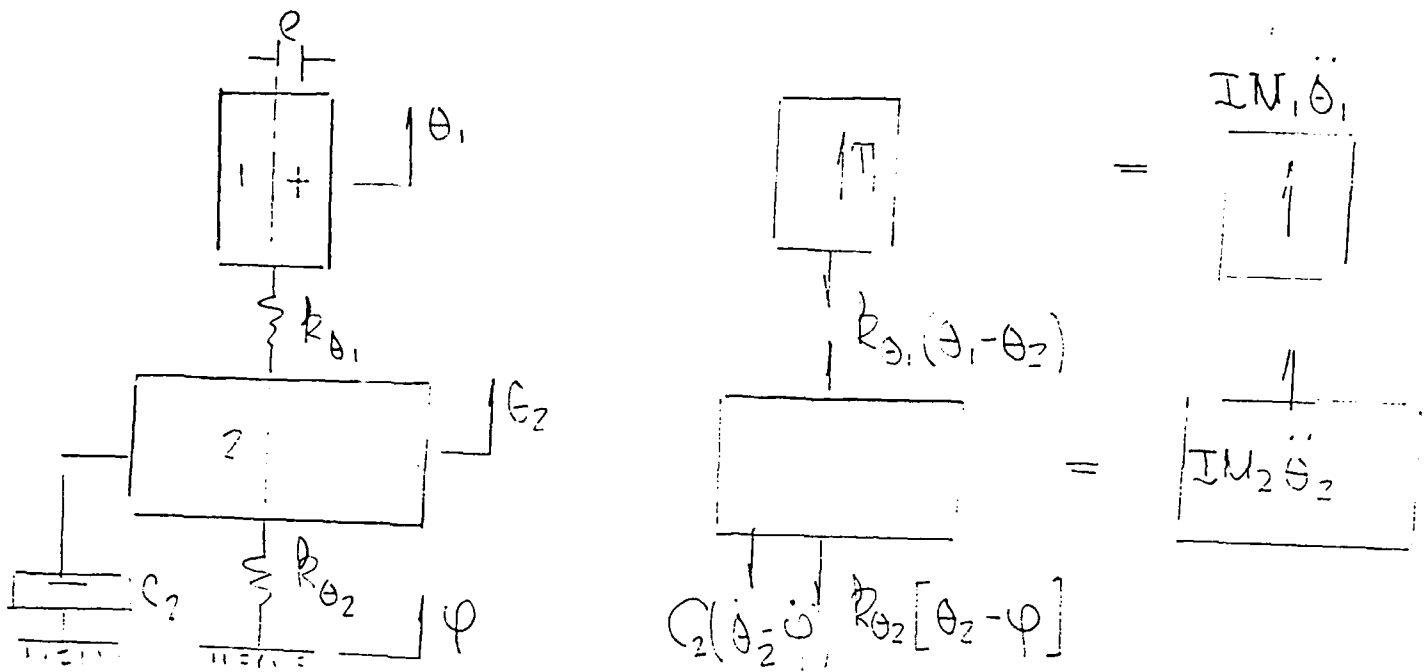
The natural frequencies of the assembly are 1.9 HZ and 29 HZ which represent the isolation system and shaft/disk assembly respectively. The eigenvalues and eigenvectors computed for each mode indicate that the isolation system is working effectively to uncouple the dynamic behavior of the structure from the ground

input. For a ground input of say 10 HZ one can expect approximately 95% isolation. Hence the table motion will be about 5% of the ground motion. The fact that the 1.9 HZ frequency is significantly uncoupled from the 29 HZ shaft/disk mode indicates that no amplification will occur between the table and the shaft. The response of the optical synchro should not be appreciably different from ground frequencies ranging from 5 to 15 HZ. Hence, as long as ground frequencies lie within these bounds, one need only worry about the amplitude of ground motion.

## 5.0 DETAIL CALCULATION.

The following pages show the detailed calculations of the analysis. The results are presented in the form of a graph (see Figure 5-2) where the absolute angular ground motion is plotted as the ordinate and the absolute horizontal ground motion as the abscissa. An error of 0.1 micro-inch is represented by a solid straight line which connects the maximum allowable angular ground rotation (radians) with the maximum allowable horizontal ground motion. Since the idealized ground motion can be represented as a linear combination of an angular rotation and a uniform horizontal displacement, the graph can be used to evaluate the expected behavior of the optical synchro.





THE TORQUE  $T_1 = M_1 \ddot{x}_2 e$  ; where  $e$  is the unit vector and  $\ddot{x}_2$  is the acceleration of the table due to a lateral ground motion.

### EQUATIONS OF MOTION

$$I_{M_1} \ddot{\theta}_1 = -k_{\theta 1} [\theta_1 - \theta_2] + T_1 \quad -1$$

$$I_{M_2} \ddot{\theta}_2 = k_{\theta 1} [\theta_1 - \theta_2] - c_2 [\dot{\theta}_2 - \dot{\varphi}] - k_{\theta 2} [\theta_2 - \varphi] \quad -2$$

LET  $z_1 = \theta_1 - \varphi \quad -3$

$z_2 = \theta_2 - \varphi \quad -4$

(2)

IT FOLLOWS THAT :

$$\begin{aligned}
 & \begin{bmatrix} I_{m_1} & 0 \\ 0 & I_{m_2} \end{bmatrix} \begin{Bmatrix} \ddot{\theta}_1 \\ \ddot{\theta}_2 \end{Bmatrix} + \begin{bmatrix} 0 & 0 \\ 0 & C_2 \end{bmatrix} \begin{Bmatrix} \dot{\theta}_1 \\ \dot{\theta}_2 \end{Bmatrix} + \begin{bmatrix} k_{\theta_1} & -k_{\theta_1} \\ -k_{\theta_1} & (k_{\theta_1} + k_{\theta_2}) \end{bmatrix} \begin{Bmatrix} \theta_1 \\ \theta_2 \end{Bmatrix} \\
 & = \begin{bmatrix} T_1 \\ 0 \end{bmatrix} - \begin{bmatrix} I_{m_1} & 0 \\ 0 & I_{m_2} \end{bmatrix} \begin{Bmatrix} 1 \\ 1 \end{Bmatrix} \ddot{\varphi} - \ddot{x}_2
 \end{aligned}$$

NOTATION : DYNAMIC PARAMETERS

$I_{m_1}$  - MASS MOMENT OF INERTIA OF SHAFT & DISK

$I_{m_2}$  - MASS MOMENT OF TABLE, CORNER WGTs AND INSTRUMENT HOUSING

$C_2$  - DAMPING OF AIR PISTONS

$k_{\theta_1}$  - TORSIONAL STIFFNESS OF BELLOWs

$k_{\theta_2}$  - TORSIONAL STIFFNESS OF ISOLATION SYSTEM

$T_1$  - TORQUE DUE TO ECCENTRICITY,  $e$ , AND LATERAL GROUND MOTION

$\ddot{\varphi}$  - ANGULAR ACCELERATION OF GROUND

$\ddot{x}_2$  - LATERAL ACCELERATION OF TABLE AND INSTRUMENT DUE TO GROUND MOTION.

## PROCEDURE

2

- (1) EVALUATE DYNAMIC PARAMETERS
- (2) COMPUTE EIGENVALUES AND EIGENVECTORS
- (3) PRE AND POST MULTIPLY EQUATION 5 TO UNCOUPLE EQUATION. [USING EIGENVECTORS COMPUTED IN STEP 2.]
- (4) SOLVE THE UNCOUPLED SETS FOR AND ASSUMED GROUPO MOTION;  $\psi = \psi_0 \sin \pi t$

EVALUATE DYNAMIC PARAMETERS

## 1.) MASS MOMENT OF INERTIA OF SHAFT AND DISK

$$(2) \text{ DISK} \approx \text{CIRCULAR PLATE} \quad D = 8.625''$$

$$t = .1875''$$

$$I_D = \frac{1}{2} m R^2$$

$$m = \pi R^2 t \rho = \pi (4.3125)^2 (.1875) (.3) = 3.286 \text{ LBS.}$$

$$I_D = \frac{1}{2} [3.286] [4.3125]^2 = 30.56 (\#-in^2)$$

$$I_{\text{SHAFT}} = \frac{1}{2} m_s r^2$$

$$m_s = \pi r^2 h \rho = \pi (1.25)^2 (7) (.3) = 10.3 \text{ LBS.}$$

$$I_{\text{SHAFT}} = \frac{1}{2} [10.3] [1.25]^2 = 8.04 (\#-in^2)$$

$$I_{M_1} = 2I_D + I_{\text{SHAFT}} = 2[30.56] + 8.04$$

$$I_{M_1} = 69.2 (\#-in^2) \quad \leftarrow$$

$$\boxed{I_{M_1} \approx 70 \#-in^2}$$

## 2) MASS MOMENT OF INERTIA OF TABLE, WEIGHTS AND INSTRUMENT

$$\text{TABLE} \sim 23'' \times 34'' \sim 150 \text{ LBS.}$$

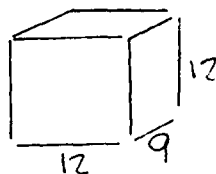
$$I_{\text{TABLE}} = \frac{1}{2} m [a^2 + b^2] = \frac{150}{2} [23^2 + 34^2]$$

$$I_{\text{TABLE}} = 126375 (\#-in^2)$$

(5)

MASS MOMENT OF INERTIA CONT'S

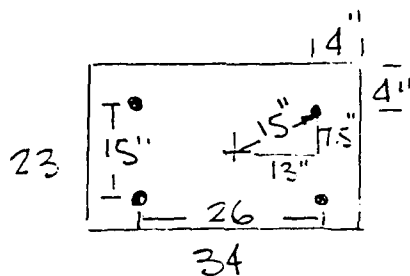
INSTRUMENT ~



$$\begin{aligned}\text{ESTIMATED } W_{GT} &= [12 \times 12 \times \frac{1}{4} \times .3]^2 + [9 \times 12 \times \frac{1}{4} \times .3]^2 4 \\ &= 21.6 + 32.4 \approx 54 \text{ LBS} \\ &\approx \text{SAY } 75 \text{ LBS.}\end{aligned}$$

$$I_{\text{BOX}} = \frac{m}{2} [a^2 + b^2] = \frac{75}{2} [12^2 + 9^2] \approx 8500 \text{ in}^2 \#$$

WGTS ~ (4) 80 LBS WGTS ARE LOCATED ON TABLE  
4" FROM EACH CORNER.



$$I_{\text{WGT}} = 80 [15]^2 4 = 72000 \text{ LB-in}^2$$

$$I_{M_2} = I_{\text{TABLE}} + I_{\text{INS}} + I_{\text{WGT}} = 126375 + 8500 + 72000$$

$$I_{M_2} = 206875 \text{ #-in}^2$$

$$I_{M_2} = 206875 \text{ #-in}^2$$

(6)

TORSION STIFFNESS OF BELLOWS  $R_{\theta_1}$  (KN 1640-30)

$$\frac{1}{K_{\phi}} = .034 \frac{\text{MIN}}{\text{IN-OZ}}$$

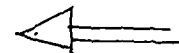
$$\frac{1}{K_{\phi}} = .034 \frac{\text{MIN}}{\text{IN-OZ}} \times \frac{16\text{OZ}}{1\text{LB}} \times \frac{60\text{SEC}}{1\text{MIN}} = 32.64 \frac{\text{SEC}}{\text{IN}\#}$$

$$4.85 \times 10^{-6} \text{ RADIANS} = 1 \text{ SEC}$$

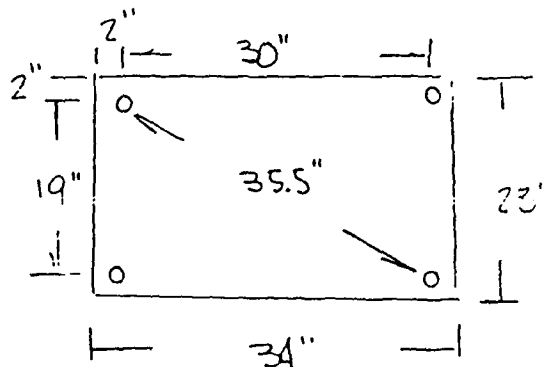
$$\frac{1}{K_{\phi}} = 32.64 \frac{\text{SEC}}{\text{IN}\#} \times \frac{4.85 \times 10^{-6} \text{ RAD}}{\text{SEC}} = 0.00015824 \frac{\text{RAD}}{\text{IN}\#}$$

$$K_{\phi} = 6320 \frac{\text{IN}\#}{\text{RADIAN}}$$

$$R_{\theta_1} = 6320 \frac{\text{IN}\#}{\text{RAD}}$$



TORSION STIFFNESS OF ISOLATION SYSTEM



# TORSIONAL STIFFNESS OF ISOLATION SYSTEM (CONT'D)

(7)

COMPUTE LATERAL STIFFNESS

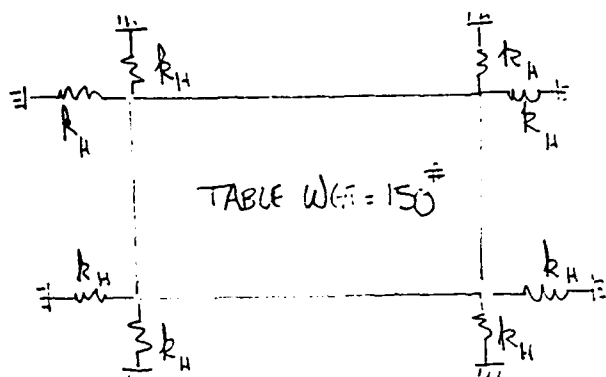
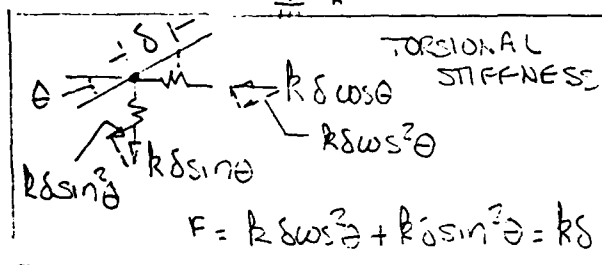


TABLE WT = 150 #



(VERTICAL MODE)

VERTICAL MODE

RESONANT FREQUENCY = 2 Hz  
(FROM MICRO-G DATA)

$$f = \frac{1}{2\pi} \sqrt{\frac{4k_g}{W}}$$

$$f^2 = \frac{1}{4\pi^2} \cdot \frac{4k_g}{W}$$

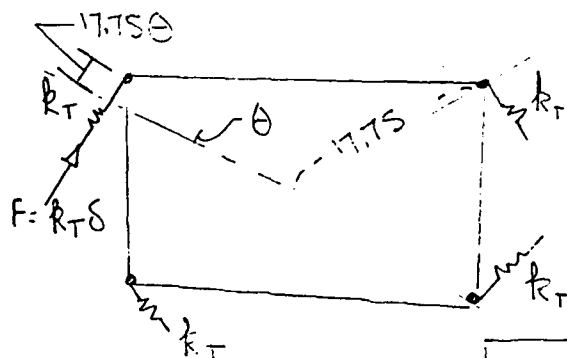
$$k_g = \frac{4\pi^2 f^2 W}{4g} = \frac{\pi^2 (2)^2 (150)}{386} = 15.34 \text{ #/in}$$

HORIZONTAL MODE ~ STIFFER THAN VERTICAL MODE;  $\frac{P}{H} \approx 4 \text{ Hz}$

$$k_H = \frac{\pi^2 P^2 W}{g} = \frac{\pi^2 (4)^2 (150)}{386} = 61.36 \text{ #/in}$$

$$k_{TOR} = k_H = 61.36 \text{ #/in (TORSIONAL)}$$

USE  $k_{TORSIONAL} = 62 \text{ #/in}$  ~ PER SPRING



$$M_T = (17.75\theta) k_T (4) (17.75)$$

$$\frac{M_T}{\theta} = (17.75)^2 (4) k_T$$

$$k_T = \frac{M_T}{\theta} = (17.75)^2 (4) (62) = 78000 \frac{\text{in} \cdot \text{#}}{\text{RAD}}$$

TORSIONAL STIFFNESS OF ISOLATOR =  $k_{\theta} = 78000 \frac{\text{in} \cdot \text{#}}{\text{RAD}}$   
LATERAL STIFFNESS OF ISOLATOR =  $k_x = 248 \text{ #/in}$

EVALUATE

UNDAMPED NATURAL FREQUENCIES OF SYSTEM  
TORSIONAL MODE.

(8)

REF PG 2

$$\omega^2 M X = K X$$

$$\frac{\omega^2}{g} \begin{bmatrix} 70 & 0 \\ 0 & 210000 \end{bmatrix} \begin{bmatrix} \theta_1 \\ \theta_2 \end{bmatrix} = \begin{bmatrix} 6320 & -6320 \\ -6320 & 84320 \end{bmatrix} \begin{bmatrix} \theta_1 \\ \theta_2 \end{bmatrix}$$

$$\frac{\omega^2}{g} \begin{bmatrix} \theta_1 \\ \theta_2 \end{bmatrix} = \begin{bmatrix} \frac{6320}{70} & -\frac{6320}{70} \\ -\frac{6320}{210000} & \frac{84320}{210000} \end{bmatrix} \begin{bmatrix} \theta_1 \\ \theta_2 \end{bmatrix}$$

$$\frac{\omega^2}{g} \begin{bmatrix} \theta_1 \\ \theta_2 \end{bmatrix} = \begin{bmatrix} 90.286 & -90.286 \\ -0.0301 & 0.4015 \end{bmatrix} \begin{bmatrix} \theta_1 \\ \theta_2 \end{bmatrix}$$

LET  $\lambda = \frac{\omega^2}{g}$

$$\begin{vmatrix} (90.29 - \lambda) & -90.29 \\ -0.0301 & (0.4015 - \lambda) \end{vmatrix} = 0$$

$$(90.29 - \lambda)(0.4015 - \lambda) - 2.717 = 0$$

$$36.2535 - 90.692\lambda + \lambda^2 - 2.717 = 0$$

$$\lambda^2 - 90.692\lambda + (45.346)^2 = -33.537 + (45.346)^2$$

$$(\lambda - 45.346)^2 = 2622.72$$

$$\lambda - 45.346 = \pm 51.214$$

$$\lambda = 96.56$$

$$\lambda = -5.868$$

$$\lambda = 1.9 \text{ rad/s}^2$$

$$\lambda = 0.22 \text{ rad/s}^2$$



(9)

FORM EIGENVECTORS

$$\lambda_1 = 0.371$$

$$\lambda_2 = 90.32$$

$$\frac{\omega^2}{g} M X = K X$$

$$\lambda \begin{bmatrix} 70 & 0 \\ 0 & 210000 \end{bmatrix} \begin{Bmatrix} \theta_1 \\ \theta_2 \end{Bmatrix} = \begin{bmatrix} 6320 & -6320 \\ -6320 & 84320 \end{bmatrix} \begin{Bmatrix} \theta_1 \\ \theta_2 \end{Bmatrix}$$

MODE 1

$$\lambda_1 = 0.3713$$

$$25.97 \theta_1 = 6320 \theta_1 - 6320 \theta_2$$

$$\text{LET } \theta_2 = 1$$

$$\theta_1 = \frac{6320}{(6320 - 25.97)} = \frac{6320}{6294} = 1.004$$

$$\boxed{\begin{matrix} \theta_1 = 1 \\ \theta_2 = .995887 \end{matrix}}$$

first modeMODE 2

$$\lambda_2 = 90.318$$

$$6322.4 \theta_1 = 6320 \theta_1 - 6320 \theta_2$$

$$\text{LET } \theta_1 = 1$$

$$\theta_2 = \frac{6320 - 6322.4}{6320} = -0.000335$$

$$\boxed{\begin{matrix} \theta_1 = 1 \\ \theta_2 = -0.000335 \end{matrix}}$$

EIGENVECTOR MATRIX

$$\Phi = \begin{bmatrix} 1 & 1 \\ .995887 & -.000335 \end{bmatrix}$$

$$M_g = \Phi^T M \Phi = \begin{bmatrix} 1 & .995887 \\ 1 & -.000335 \end{bmatrix} \begin{bmatrix} 70 & 0 \\ 0 & 210000 \end{bmatrix} = \begin{bmatrix} 70 & 209136.3 \\ 70 & -70.35 \end{bmatrix}$$

$$M_g = \begin{bmatrix} 70 & 209136.3 \\ 70 & -70.35 \end{bmatrix} \begin{bmatrix} 1 & 1 \\ .995887 & -.000335 \end{bmatrix} = \begin{bmatrix} 208300 & 0 \\ 0 & 70.02 \end{bmatrix}$$

$$K_g = \Phi^T K \Phi = \begin{bmatrix} 1 & .995887 \\ 1 & -.000335 \end{bmatrix} \begin{bmatrix} 6320 & -6320 \\ -6320 & 84320 \end{bmatrix} = \begin{bmatrix} 25.994 & 77652 \\ 6322.1 & -6348.7 \end{bmatrix}$$

$$K_g = \begin{bmatrix} 25.994 & 77652 \\ 6322.1 & -6348.7 \end{bmatrix} \begin{bmatrix} 1 & 1 \\ .995887 & -.000335 \end{bmatrix} = \begin{bmatrix} 77359.6 & 0 \\ 0 & 6324.2 \end{bmatrix}$$

$$\Phi^T M = \begin{bmatrix} 70 & 209136.3 \\ 70 & -70.35 \end{bmatrix} \begin{Bmatrix} 1 \\ 1 \end{Bmatrix} = \begin{bmatrix} 209206 \\ -.35 \end{bmatrix}$$

(11)

IGNORE HORIZONTAL DAMPING  $[c = 0]$ PARTICIPATION FACTORS

$$\gamma_1 = \frac{209206}{208300} = 1.004$$

$$\gamma_2 = -\frac{.35}{70.02} = -.004128$$

EQUATIONS OF MOTION

$$\frac{1}{g} \begin{bmatrix} 208300 & 0 \\ 0 & 70.02 \end{bmatrix} \begin{Bmatrix} \ddot{\eta}_1 \\ \ddot{\eta}_2 \end{Bmatrix} + \begin{bmatrix} 77359.6 & 0 \\ 0 & 6324.2 \end{bmatrix} \begin{Bmatrix} \eta_1 \\ \eta_2 \end{Bmatrix}$$

$$= \begin{bmatrix} 1 & .995887 \\ 1 & -.000335 \end{bmatrix} \begin{Bmatrix} T_1 \\ 0 \end{Bmatrix} - \frac{1}{g} \begin{Bmatrix} 209206 \\ -0.35 \end{Bmatrix} \ddot{\psi}$$

WHERE ;

$$\begin{Bmatrix} z_1 \\ z_2 \end{Bmatrix} = \begin{bmatrix} 1 & 1 \\ .995887 & -.000335 \end{bmatrix} \begin{Bmatrix} \eta_1 \\ \eta_2 \end{Bmatrix}$$

EQUATION UNCOUPLED1ST MODE

$$\frac{208300 \ddot{\eta}_1 + 77359.6 g \eta_1}{\ddot{\eta}_1 + .371389 \ddot{\psi}} = \frac{T_1}{208300} - 1.004 \ddot{\psi}$$

2nd mode

$$10.02 \ddot{\eta}_2 + 6324.2 \eta_2 = 9T_1 + 0.35 \ddot{\varphi}$$

$$\boxed{\ddot{\eta}_2 + 90.379 \eta_2 = \frac{9T_1}{10.02} + .004128 \ddot{\varphi}}$$

Solve for  $\eta_1$  &  $\eta_2$

$$\ddot{\eta}_1 + .37138(386) \eta_1 = \frac{386}{208300} T_1 - 1.004 \ddot{\varphi}$$

$$\ddot{\eta}_1 + 143.353 \eta_1 = 0.0018531 T_1 - 1.004 \ddot{\varphi}$$

Assume;  $\varphi = \varphi_0 \sin \pi t$

$$\ddot{\varphi} = -\varphi_0 \pi^2 \sin \pi t$$

$$\eta_1 = A_0 \sin \pi t + \eta_0$$

$$-A_0 \pi^2 \sin \pi t + 143.353 [A_0 \sin \pi t + \eta_0] = 0.0018531 T_1 + 1.004 \varphi_0 \pi^2 \sin \pi t$$

$$-A_0 \pi^2 + 143.353 A_0 = 1.004 \varphi_0 \pi^2$$

$$143.353 \eta_0 = 0.0018531 T_1$$

(13)

$$A_0 = \frac{1.004 \phi_0 \eta^2}{[143.353 - \eta^2]}$$

$$\eta_{10} = \frac{0.0018531 T_1}{143.353}$$

$$\eta_1 = \frac{1.004 \phi_0 \eta^2}{[143.353 - \eta^2]} \sin \pi t + \frac{0.0018531 T_1}{143.353}$$

Solve for  $\eta_2$

$$\ddot{\eta}_2 + 90.32(386) \eta_2 = \frac{T_1(386)}{70.02} - 0.00412 \phi_0 \eta^2 \sin \pi t$$

$$\ddot{\eta}_2 + 34863.52 \eta_2 = 5.5127 T_1 - 0.00412 \phi_0 \eta^2 \sin \pi t$$

$$\eta_2 = B_0 \sin \pi t + \eta_{20}$$

$$-B_0 \eta^2 \sin \pi t + 34863.52 [B_0 \sin \pi t + \eta_{20}] = 5.5127 T_1 - 0.00412 \phi_0 \eta^2 \sin \pi t$$

$$-B_0 \eta^2 + 34863.52 B_0 = -0.00412 \phi_0 \eta^2$$

$$34863.52 B_0 = 5.5127 T_1$$

$$B_0 = - \frac{0.00412 \phi_0 \pi^2}{[34863.52 - \pi^2]}$$

$$\eta_{20} = \frac{5.5127 T_1}{34863.52}$$

RELATIVE MOTION OF DISK AND FOULING

$$\begin{aligned} \theta_1 - \theta_2 &= z_1 - z_2 = [\eta_1 + \eta_2 - (.99588 \eta_1 - .000335 \eta_2)] \\ &= 0.004113 \eta_1 + 1.000335 \eta_2 \end{aligned}$$

$$\begin{aligned} [\theta_1 - \theta_2] &= 0.004113 \left\{ \left[ \frac{1.004 \phi_0 \pi^2}{(143.353 - \pi^2)} \right] \sin \pi t + \frac{0.0018521 T_1}{143.353} \right\} \\ &+ 1.000335 \left\{ \left[ - \frac{.00412 \phi_0 \pi^2}{(34863.52 - \pi^2)} \right] \sin \pi t + \frac{5.5127 T_1}{34863.52} \right\} \end{aligned}$$

$$|\theta_1 - \theta_2|_{\max} = \left[ \frac{.004129 \pi^2}{[143.353 - \pi^2]} - \frac{.004121 \pi^2}{[34863.52 - \pi^2]} \right] \phi_0 + 0.00015822 T_1$$

MAXIMUM RELATIVE MOTION  $|\theta_1 - \theta_2|$

$$|\theta_1 - \theta_2| = \left[ \frac{.004129 \pi^2}{143.353 - \pi^2} - \frac{0.004121 \pi^2}{34863.52 - \pi^2} \right] \phi_0 + 0.00015823 T_1$$

Assume GROUND FREQUENCY = 10 Hz

$$\pi = 2\pi 10 = 20\pi = 62.83$$

$$\pi^2 = 3947.8$$

$$\pi = 10 \text{ Hz}$$

$$|\theta_1 - \theta_2| = [-.0042846 - .00052623] \phi_0 + 0.00015823 T_1$$

$$\theta_{REL} = .004811 \phi_0 + 0.00015823 T_1 \quad \text{--- (a)}$$

Assume GROUND FREQUENCY = 5 Hz

$$\pi = 31.416$$

$$\pi^2 = 986.96$$

$$\theta_{REL} = [-0.00483 - .00012] \phi_0 + 0.00015823 T_1$$

$$\theta_{REL} = .00495 \phi_0 + 0.00015823 T_1 \quad \text{--- (b)}$$

(16)

$$\text{GROUND MOTION} = 15 \text{ Hz}$$

$$\pi = 94.2477$$

$$M^2 = 888.64$$

$$\Theta_{REL} = [0.001197 + 0.0014] \phi_0 + 0.00015833 T_1$$

$$\Theta_{REL} = 0.0056 \phi_0 + 0.00015833 T_1 \quad \text{--- C}$$

$$\text{ERROR} = \Theta_{REL} \times R = [0.001811 \phi_0 + 0.00015833 T_1] 4.3$$

$$\boxed{\text{ERROR} = 0.0207 \phi_0 + 0.00068 T_1} \quad @ \quad \pi = 10 \text{ Hz}$$

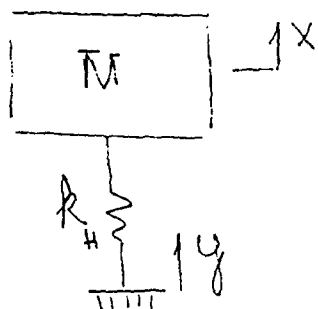
$$T_1 = M_1 \ddot{X}_1 e$$

$$M_1 = M_{DISK} + M_{SHAFT} = (3.286)2 + 8.04 = 14.61 \text{ LBS.}$$

$$\begin{aligned} \text{GROUND MOTION: } X &= X_0 \sin \pi t \\ \ddot{X} &= -X_0 \pi^2 \sin \pi t \\ \ddot{X}_{MAX} &= -X_0 \pi^2 \end{aligned}$$



# HORIZONTAL GROUND MOTION



$$M_{\text{ASS}} = W_{\text{TABLE}} + W_{\text{BOX}} + W_{\text{INST}} \\ = 150 + 4(80) + [2(3.3) + 10.2 + 75]$$

$$W_{\text{TOT}} = 562 \text{ LBS.}$$

$$k_H = 62 \frac{\text{#}}{\text{in}} (4) = 248 \frac{\text{#}}{\text{in}}$$

$$\frac{1}{f} = \frac{1}{2\pi} \sqrt{\frac{248(386)}{562}} = 2.08 \text{ Hz}$$

$$M\ddot{x} + k(x-y) = 0$$

$$M\ddot{x} + kx = ky$$

$$\ddot{x} + \omega^2 x = \omega^2 y$$

ASSUME GROUND MOTION IS SINUSOIDAL  
OF THE FORM  $y = y_0 \sin \omega t$

then  $x = x_0 \sin \omega t$ .

SUBSTITUTION YIELDS

$$-M^2 x_0 + \omega^2 x_0 = \omega^2 y_0$$

$$x_0 = \frac{\omega^2 y_0}{\omega^2 - \mu^2} = \frac{y_0}{1 - \frac{\mu^2}{\omega^2}}$$

FOR A GROUND INPUT @  $10 \text{ Hz}$ ; THE EXPECTED TABLE MOTION IS

$$X_0 = \frac{Y_0}{\left[1 - \left(\frac{10}{2.08}\right)^2\right]} = 0.045 Y_0$$

CONCLUSION: APPROXIMATELY  $1/20$  OF THE GROUND MOTION GET TO THE TABLE TOP.

THE ACCELERATION OF THE TABLE TOP / INSTRUMENT IS;

$$\ddot{X} = X_0 \pi^2 = \frac{Y_0 \pi^2}{\left[1 - \left(\frac{\pi}{\omega}\right)^2\right]}$$

THE TORQUE PRODUCED ON THE SHAFT FOR AN UNBALANCED SYSTEM OF ECCENTRICITY,  $e$  IS

$$T = M_{SH} \ddot{X} e = \frac{[2(3.3) + 10.3]}{g} \cdot \frac{Y_0 \pi^2 e}{\left[1 - \left(\frac{\pi}{\omega}\right)^2\right]}$$

$$\text{Torque} = \frac{16.9}{386} \cdot \frac{Y_0 \pi^2 e}{\left[1 - \left(\frac{\pi}{\omega}\right)^2\right]} = 0.0438 \frac{\pi^2}{\left[1 - \left(\frac{\pi}{\omega}\right)^2\right]} Y_0 e$$

$$T \approx 0.0438 \frac{\pi^2 e}{\left[1 - \left(\frac{\pi}{\omega}\right)^2\right]} Y_0 \sin \omega t$$

17

SINCE THE TORQUE IS APPLIED SIMULTANEOUSLY  
AT THE FREQUENCY OF THE TABLE WHICH RESPONDS  
AT  $\approx 2 \text{ Hz}$  IT MAY BE TREATED AS A SLOWLY  
APPLIED <sup>(STATIC)</sup> LOAD RELATIVE TO THE FREQUENCY OF  
THE SHAFT (20 Hz).

$$\text{HENCE } T_{\text{STATIC}} = 0.0438 \frac{\gamma^2}{\left[1 - \left(\frac{\pi}{\omega}\right)^2\right]} \gamma_0 e$$

Q  $\pi = 10 \text{ Hz}$   
 $\omega = 2.08 \text{ Hz}$

$$T_{\text{STATIC}} = 0.0438 \frac{[2\pi(10)]^2}{\left[1 - \left(\frac{10}{2.08}\right)^2\right]} \gamma_0 e$$

$$\boxed{T_1 = 7.819 \gamma_0 e}$$

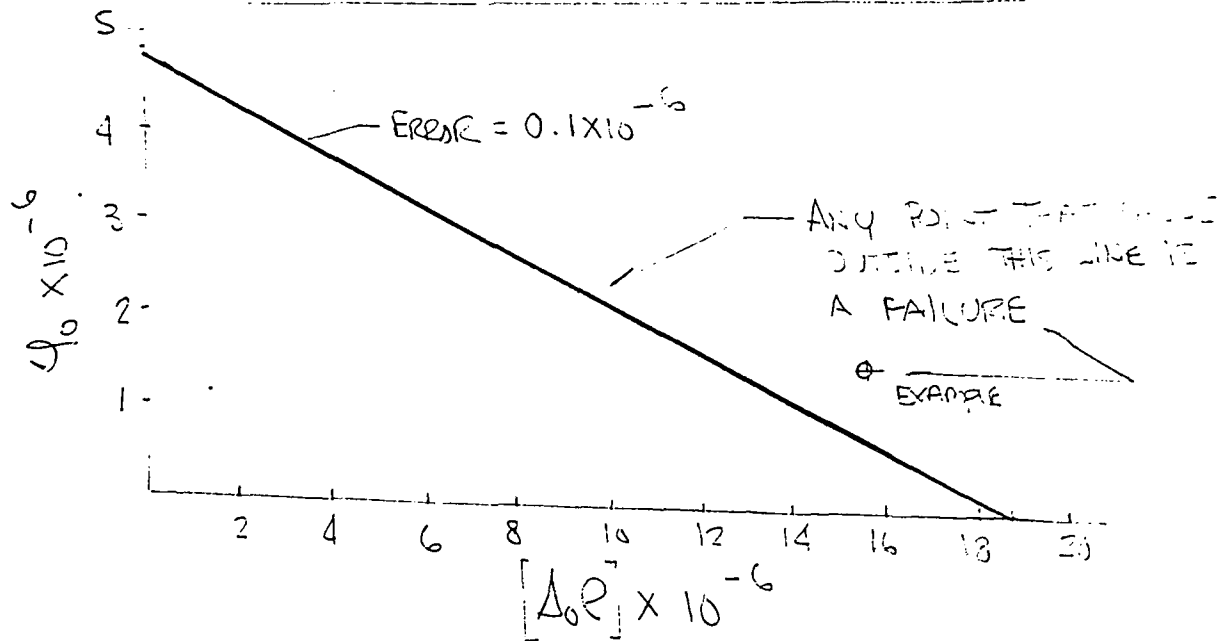
$$\text{ERROR} = 0.0207 \phi_0 + 0.00068 [7.819 \Delta_0 e]$$

$$\boxed{\text{ERROR} = 0.0207 \phi_0 + 0.00532 \Delta_0 e} \quad \text{Q } 10 \text{ Hz}$$

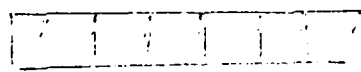
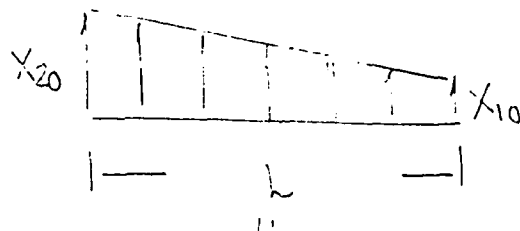
SET ERROR =  $0.1 \times 10^{-6}$  ALLOWABLE

$0.1 \times 10^{-6} = 0.0207 \phi_0 - 0.00532 \Delta_0 R$

$\phi_0 = 4.83 \times 10^{-6} - 0.257 [\Delta_0 R]$



GROUND MOTION - GENERAL



$\Delta_0 = \frac{X_{20} + X_{10}}{2}$

# OPTRALITE™ 2-FREQUENCY LASER

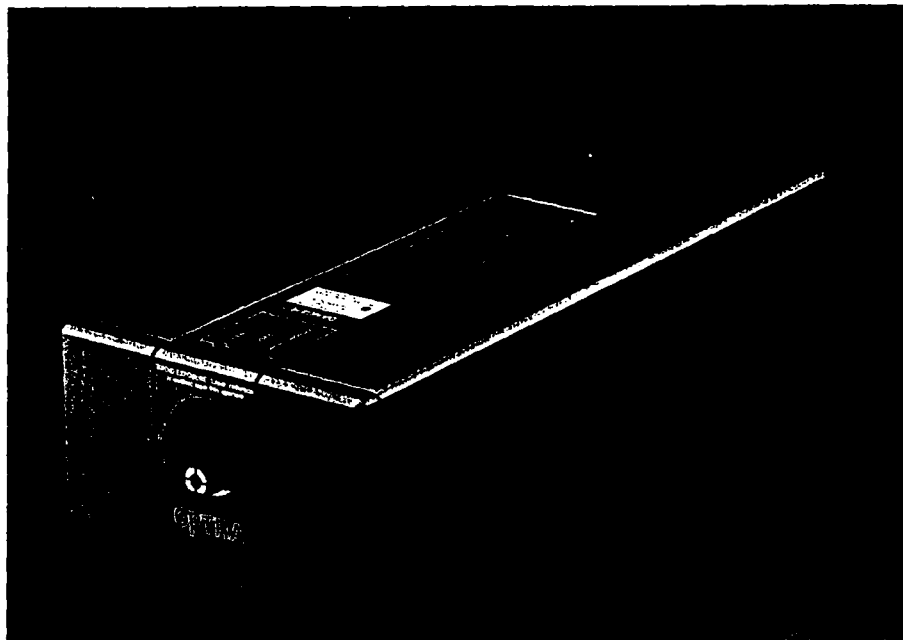
## Product Highlights

- 2-Frequency Output.
- Highly Stabilized Optical Frequency.
- Small, Self-Contained Unit.
- System Compatible.
- High Performance - Low Cost.

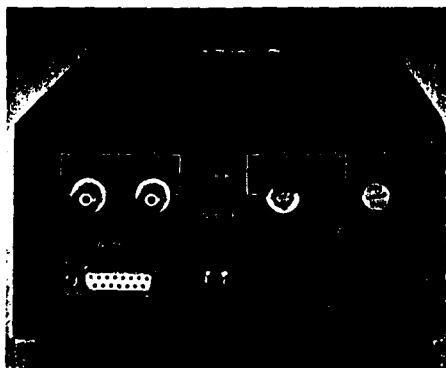
The OPTRALITE™ laser is a new, high performance component designed for use in critical measuring applications. This HeNe laser delivers a stabilized, 2-frequency output that is well suited for linear metrology and other measuring techniques. Unique design features provide the user with the following product capabilities:

**2-Frequency Output:** The OPTRALITE laser produces a collimated, 2-frequency, Zeeman-split output which is ideal for interferometric measurements. The 2-frequency components are orthogonally polarized (either linear or circular polarizations), and when made to interfere, they produce a beat frequency of precisely 250 KHz. Similarly, OPTRALITE can be easily converted to a single frequency stabilized source. An interferometer, coupled with a 2-frequency laser, permits the user to make extremely accurate measurements with low noise levels, in addition to resolving the direction of movement along the measured axis.

**Highly Stabilized Optical Frequency:** OPTRALITE's highly stabilized optical frequency increases the versatility of the laser for applications utilizing either the single frequency or the 2-frequency output. The OPTRALITE output is carefully stabilized to better than one part in  $10^7$  and will maintain this stability through a significant range of environmental conditions.



**Small Self-Contained Unit:** OPTRALITE is completely self-contained in one sturdy enclosure which incorporates all of the electrical components. A built-in detector located at the front of the laser permits easy monitoring of the returning beam. These features facilitate integration into larger systems as well as handling by the end user.



Back panel design allows easy access to controls as well as connections for remote operation.

**System Compatibility:** The performance characteristics and size of OPTRALITE, make it highly compatible with other systems. The laser can be operated manually or with a microprocessor. Computer compatible outputs are included for remote controlled applications.

**High Performance/Low Cost:** Because of OPTRA's proprietary design\*, the OPTRALITE laser is able to incorporate high performance characteristics and versatile product features in a comparatively low cost unit.

See OPTRALITE specifications on reverse side.

\*Patent applied for.

## OPTRA

Cherry Hill Park

1 66 Cherry Hill Drive • Beverly, MA 01915  
(508) 921-2100 • FAX 508-921-2055

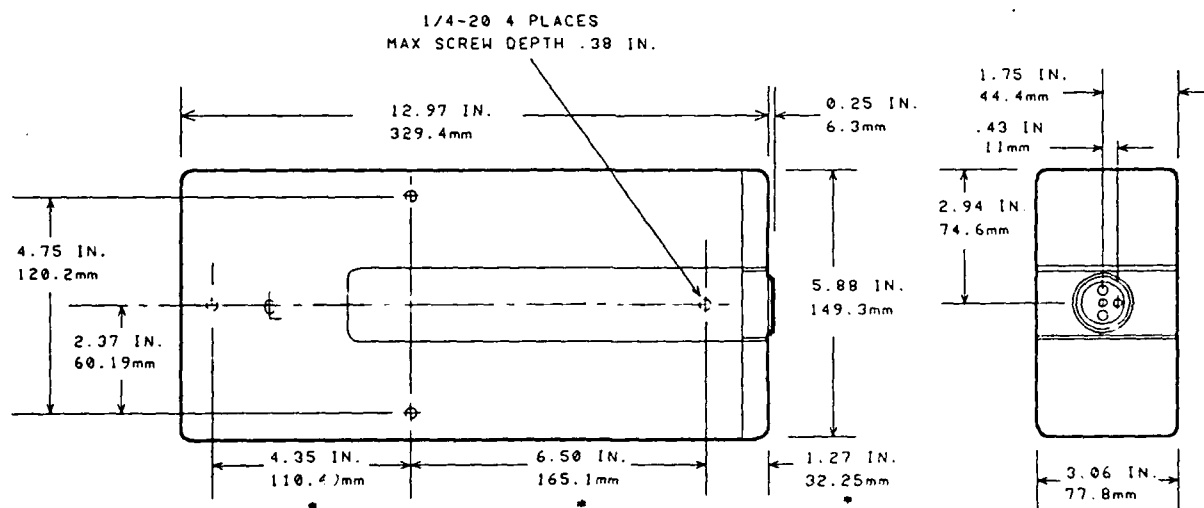
## Specifications

<b>Laser Type</b>	HeNe 2-Frequency, Stabilized, Zeeman-Split output	<b>Warm Up Time</b>	< 5 minutes
<b>Laser Wavelength</b>	632.8 nm	<b>Power Requirements</b>	115/220 VAC, 60/50 Hz 40 VA avg. (65 VA peak)
<b>Output Polarization</b>	Orthogonal Linear or Orthogonal Circular*	<b>Operating Lifetime</b>	> 10,000 Hours
<b>Beat Frequency</b>	250.00 KHz	<b>Working Environment</b>	Temp: 0-40°C. (32-105°F) Rel. Hum: 0-95% (Non-condensing)
<b>Optical Frequency Stability</b>	1 part in 10 <sup>7</sup>	<b>Electrical Outputs</b>	Reference Signals, TTL Diagnostics
<b>Output Power</b>	1.0 mw. (2-Frequency Mode) 0.5 mw. (Single Frequency Mode)*	<b>Mounting</b>	1/4-20 UNC (base) Rubber pads for bench use
<b>Beam Diameter</b>	0.64 mm	<b>Safety Features</b>	Class IIIa Laser Meets NCDRH requirements shutter, remote beam on/off
<b>Beam Divergence</b>	1.27 mrad		
<b>Transverse Mode</b>	TEM <sub>00</sub>		

\*Attachments Available



## DIMENSIONS



▲ MOUNTING DIMENSIONS  
(OPPOSITE SIDE)

# OPTRA

Cherry Hill Park  
66 Cherry Hill Drive • Beverly, MA 01915  
(508) 921-2100 • FAX 508-921-2055

11/86

# OPTRAMETER™ MEASUREMENT MODULE

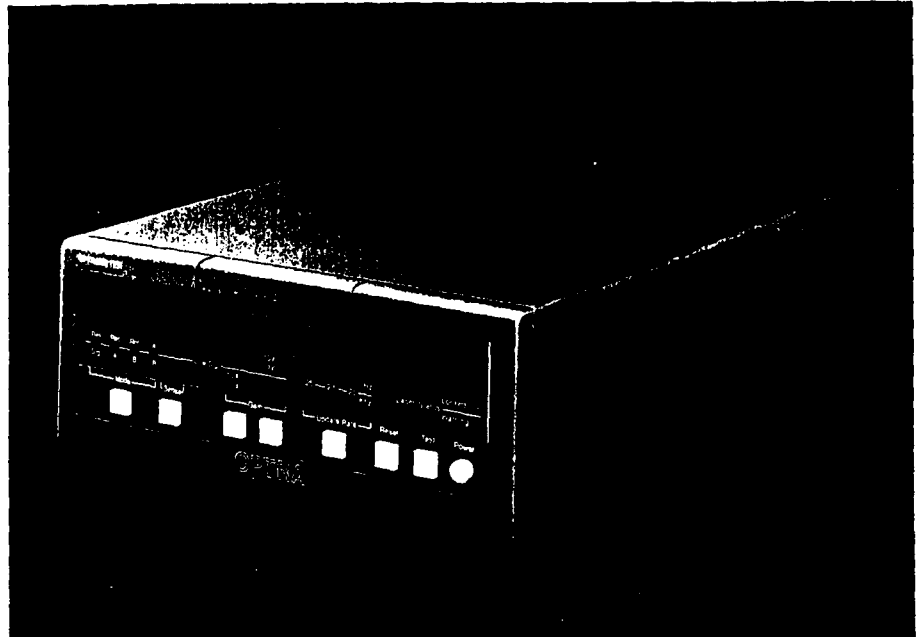
## Product Highlights

- Permits Precise Quantitative Measurements
- Selectable Features For Greater Versatility
- Several Interfaces For Unique Measurement Needs
- Practical Design For Easy Operation
- High Performance/Low Cost Unit

The OPTRAMETER™ Measurement Module is a high performance cumulative phase measuring component for critical measurement applications. When coupled with the OPTRALITE™ 2-frequency laser this product enables the user to make quantitative interferometric measurements. The primary features of the OPTRAMETER are described below:

**Permits Precise Quantitative Measurements:** The OPTRAMETER Module compares the phase angle of two signal inputs and counts each passing cycle of phase. This product will measure one thousandth of a cycle of phase. When integrated with a 2-frequency laser, the OPTRAMETER module is capable of resolving up to a 0.001 of a wavelength. This permits the user to make highly accurate, quantitative measurements for a variety of interferometric applications.

**Selectable Features For Greater Versatility:** OPTRAMETER is equipped with a number of selectable features for greater versatility and a variety of measurement needs. Mode selection allows the user to compare incoming signals from external detectors, a laser, or other sources. The selectable update rate provides fast data gathering or averaging for greater precision. An indicator monitors signal strength and the gain feature will enhance the signal when needed.



**Several Interfaces For Unique Measurement Needs:** OPTRAMETER will interface easily with a host computer for unique measurement situations. A 44 Bit parallel BCD interface provides the user with data for remote processing. OPTRAMETER is also equipped with a 9600 Baud RS232 output for interfacing with a desk top computer. The analog output is useful for monitoring data with an oscilloscope, a waveform analyzer, or an X-Y plotter.



*Front panel design permits easy accessibility for function selection and a clear view of the display.*

**Practical Design for Easy Operation:** OPTRAMETER's compact design facilitates easy use in industrial or laboratory applications. The product is completely self-contained. The back panel provides an easy access to incoming connections and detector configurations for a variety of measurement needs. The 11 digit, LED display allows easy viewing of data and the system status.

**High Performance/Low Cost Unit:** Based on OPTRA's proprietary modular design\* for the OPTRAMETER, this product provides high performance capability for a variety of interferometric measurement needs at a reasonable cost.

Please see reverse side for product specifications.

\*Patent applied for

## OPTRA

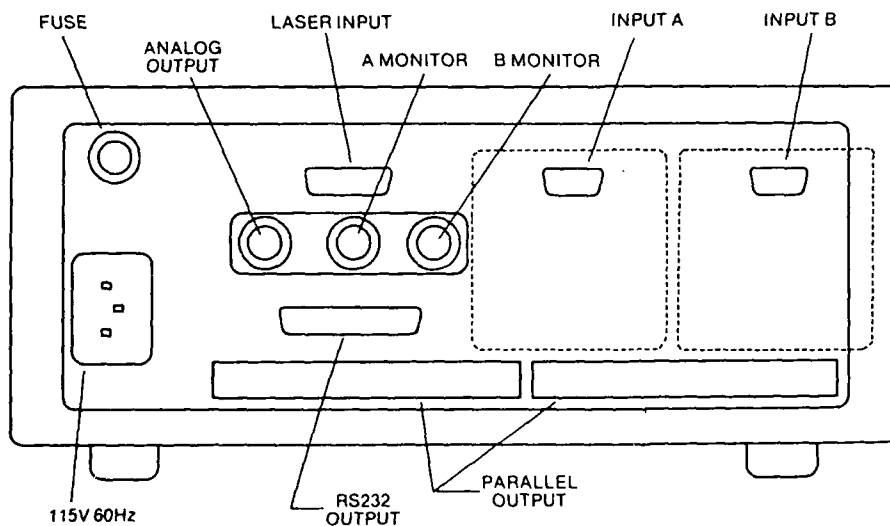
Cherry Hill Park  
66 Cherry Hill Drive • Beverly, MA 01915  
(508) 921-2100 • FAX 508-921-2055

## Specifications

<b>Measurement Accuracy</b>	< $1 \times 10^{-3}$ Cycle @ 100 Hz. < $1 \times 10^{-3}$ Cycle @ 1000 Hz.	<b>Serial Output</b>	RS232c, ASCII Format, 9600 BAUD.
<b>Measurement Range</b>	0.001 to $10^6$ cycles	<b>Analog Output</b>	$\pm 10$ VDC Range: $\pm 9.999$ cycles
<b>Input Signal Range</b>	100mV to 10V (peak to peak at 250KHz.)	<b>Display</b>	11 Digit, LED with status indicators
<b>Phase Noise</b>	< $3 \times 10^{-3}$ cycles @ 25 KHz. (peak to peak)	<b>Instrument Range</b>	- 99999999.999 to + 99999999.999
<b>Phase Drift</b>	Short Term: < $2 \times 10^{-3}$ cycles (1 min.) Long Term: < $5 \times 10^{-3}$ cycles (8 Hrs.)	<b>Power Requirements</b>	115 VAC @ 60 Hz. 25 VA avg 240 VAC @ 50 Hz. (option)
<b>Selectable Update</b>	0.25, 2.5, 25, 250 Hz. 2.5, 25 KHz.	<b>Environment</b>	Temp; +10° C to +40° C Humidity; 10% to 95% non-condensing
<b>Gain Control</b>	1X or 10X Manual Selection		
<b>Parallel Output</b>	44 Bit, BCD Format plus Sign, TTL Compatible		

Specifications for 250 KHz inputs.

## Back Panel



### Dimensions

Length of Unit — 13"  
Height of Unit — 3.80"  
with feet (for table mount) — 4.20"  
Width of Unit — 9.50"  
Weight of Unit — 8 lbs.

# OPTRA

Cherry Hill Park  
66 Cherry Hill Drive • Beverly, MA 01915  
(508) 921-2100 • FAX 508-921-2055

11/86



# APPENDIX E

## Slave-Tracking-Master Data

Master Encoder				Slave Encoder				
Run No.	Start	Angle	Return	Error	Start	Angle	Return	Error
1	2.93	320.60	2.98	+05	2.91	321.04	2.97	+06
2	2.98	329.60	2.97	-01	2.98	329.95	2.96	-02
3	2.96	322.50	3.00	+04	2.95	322.88	2.99	+04
4	3.00	344.67	3.01	+01	2.99	345.06	3.01	+02
5	2.95	334.50	3.02	+07	2.93	334.90	3.02	+09
6	2.96	323.50	2.99	+03	2.94	323.83	2.99	+05
7	2.99	339.57	2.99	0	2.98	339.97	2.98	0
8	2.98	322.70	3.01	+03	2.96	323.17	3.00	+04
9	2.97	322.16	3.01	+04	2.95	322.47	2.99	+04
10	3.04	323.60	3.04	0	3.03	323.93	3.03	0
11	3.02	348.70	3.07	+05	3.02	349.06	3.07	+05
12	3.00	340.80	3.04	+04	2.99	341.23	3.03	+04
13	3.00	340.54	3.03	+03	2.98	340.90	3.02	+04
14	2.98	326.65	3.02	+04	2.97	327.12	3.01	+04
15	3.01	314.65	3.01	0	3.00	315.13	2.99	-01
16	3.01	317.03	3.02	+01	3.01	317.47	3.02	+01
17	3.01	328.83	3.04	+03	3.01	329.32	3.04	+03
18	3.02	328.55	3.04	+02	3.02	328.97	3.03	+01
19	3.02	331.02	3.04	+02	3.02	331.52	3.05	+03
20	2.99	347.60	3.04	+05	2.98	348.00	3.05	+07
21	3.03	313.69	3.02	-01	3.04	314.00	3.03	-01
22	2.96	354.11	3.05	+09	2.96	354.45	3.07	+11
23	12.98	349.24	13.00	+02	12.98	349.74	13.01	+03
24	12.97	336.96	13.00	+03	12.97	337.46	13.00	+03
25	12.96	339.70	12.99	+03	12.96	340.08	12.99	+03
26	12.93	328.32	12.98	+05	12.94	328.71	12.98	+04
27	12.98	333.05	12.97	-01	12.98	333.54	12.98	0
28	12.96	334.60	12.99	+03	12.97	335.04	12.99	+02
29	12.96	334.20	12.98	+02	12.97	334.56	12.99	+02
30	12.96	335.75	12.98	+02	12.97	336.12	12.99	+02
31	12.97	333.30	12.98	+01	12.98	333.73	13.00	+02
32	12.95	341.03	12.98	+03	12.97	341.58	13.00	+03
33	12.96	320.50	12.96	0	12.97	320.96	12.98	+01
34	12.94	333.81	12.98	+04	12.95	334.19	12.99	+04
35	12.92	334.73	12.96	+04	12.94	335.28	12.97	+03
36	12.88	321.21	12.94	+06	12.90	321.66	12.96	+06
37	12.87	334.60	12.93	+06	12.89	335.10	12.95	+06
38	12.84	291.39	12.90	+06	12.86	291.82	12.92	+06
39	12.89	321.13	12.94	+05	12.94	321.17	12.98	+04
40	34.86	399.43	35.03	+17	34.93	400.00	35.11	+18
41	34.84	364.48	34.92	+08	34.90	365.00	34.98	+08
42	34.86	320.16	34.88	+02	34.91	320.73	34.93	+02
43	34.86	245.78	34.87	+01	34.92	246.29	34.92	0
44	34.81	303.82	34.89	+08	34.85	304.38	34.95	+10

The above data was taken at an update rate of 25 kHz.